Manufacturing of Blends based on Biopolyesters and Polylactides: Process-induced Structure and Properties

Juliana Vanessa Cardoso Azevedo, Ph.D.

Doctoral Thesis Summary

Tomas Bata University in Zlín

Tomas Bata University in Zlín
Faculty of Technology

Doctoral Thesis Summary

Zpracování PBAT/PLA směsí: vliv procesních podmínek na strukturní a užitné vlastnosti

Manufacturing of Blends based on Biopolyesters and Polylactides: Process-induced Structure and Properties

Author: **Juliana Vanessa Cardoso Azevedo, Ph.D.**

Degree programme: P 3909 Processing Engineering

Degree course: 3909V012 Tools and Processes

Supervisor: Prof. Ing. Berenika Hausnerová, Ph.D.

External examiners: Prof. Ing. Pavel Mokrejš, Ph.D.
Prof. Dr. Johannes Steinhaus

Zlín, January 2024

Published by **Tomas Bata University in Zlín** in the Edition **Doctoral Thesis Summary.**
The publication was issued in the year 2024

Key words in Czech: *poly(butylen-adipát-tereftalát); kyselina polymléčná, modifikátory délky řetězců a síťování; tokem indukovaná struktura; termomechanické vlastnosti; morfologie; rozklad kompostováním*

Key words: *poly(butylene adipate-co-terephthalate); poly(lactic acid); chain extender cross-linker; blown film extrusion; process-induced structure; thermo-mechanical properties; morphology; compost disintegration*

Full text of the doctoral thesis is available in the Library of TBU in Zlín.

ISBN 978-80-7678-228-0

RESUME IN CZECH

V disertační práci byly zkoumány zpracováním indukované změny v termomechanických a viskoelastických vlastnostech a odpovídající morfologii vyfukovaných fólií z biodegradovatelné směsi polybutylentereftalátu adipátu (PBAT) a kyseliny polymléčné (PLA) modifikované čtyřmi typy multifunkčních CECL (chain-extending cross-linkers). Zavedení CECL významně ovlivnilo vlastnosti referenční směsi PBAT/PLA. Termální analýza ukázala, že chemické reakce nebyly dokončeny během kompoundace, ale probíhaly i během zpracování směsi vytlačovacím vyfukováním. SEM analýzy lomových povrchů vyfukovaných filmů odhalily významný vliv CECL na morfologii vytvořenou během zpracování i na degradační procesy. Navíc se reakce CECL s PBAT/PLA anizotropická - liší ve směru souběžném a kolmém na směr vyfukování. Pomocí změny rozfukovacího poměru byla zkoumána synergie mezi mechanickými a morfologickými vlastnostmi modifikovaných směsí. U vytlačovacího vyfukování je důležitá znalost elongační viskozity. Její stanovení pro PBAT/PLA je však na SER reometru značně problematické, proto byl vypracován nový postup hodnocení deformačního chování v tahu pro biodegradabilní alternativy syntetických polyolefinů.

RESUME

Process-induced changes in thermo-mechanical viscoelastic properties and the corresponding morphology of biodegradable polybutylene adipate terephthalate (PBAT) and polylactic acid (PLA) blown film blends modified with four multifunctional chain-extending cross-linkers (CECL) were investigated. The introduction of CECL modified the properties of the reference PBAT/PLA blend significantly. The thermal analysis showed that the chemical reactions were incomplete after compounding, and that film blowing extended them. SEM investigations of the fracture surfaces of blown extrusion films reveal the significant effect of CECL on the morphology formed during the processing. The anisotropic morphology introduced during film blowing proved to affect the degradation processes as well. Furthermore, the reactions of CECL with PBAT/PLA induced by the processing depend on the deformation directions. The blow-up ratio parameter was altered to investigate further process-induced changes proving synergy with mechanical and morphological features. Using blown film extrusion, the elongational behavior represents a very important characteristic. However, its evaluation may be quite often problematic, but with the SER Universal Testing Platform it was possible to determine changes in the duration of time intervals corresponding to the rupture of elongated samples.

TABLE OF CONTENT

1. Introduction

The global plastic waste problems positively affected the development of biodegradable polymers and other sustainable materials [1-4] towards substitution of traditional packaging plastics such as polyethylene (PE) and polystyrene (PS) by biodegradable starch and biopolyesters [5-7]. The term biopolymer summarizes three classes of polymers:

1. Polymers that are biodegradable but do not necessarily stem from renewable resources e.g. poly(butylene adipate-co-terephthalate) (PBAT), polycaprolactone (PCL);
2. Polymers that stem from renewable resources directly e.g. polylactic acid (PLA), Polyhydroxyalkanoate (PHA);
3. Polymers that are synthesized using monomers of biological origin but are not biodegradable e.g. polyamide 6 (PA 6) from sebacic acid, PE from sugar cane.

However, for more demanding engineering applications and to accelerate the conversion to a circular economy, their mechanical properties must be enhanced without compromising their biodegradability. Many biopolymers are blended with other polymers to balance the properties required for specific applications: PLA often exhibits a brittle behavior and is inappropriate for applications requiring high deformation strains [8-9]. Therefore, blending with ductile polymers such as PBAT appears to be a reasonable approach. Often, mineral fillers, e.g. calcium carbonate or talc, are added to a blend to optimize its stiffness and permeation properties [10-12].

The compatibilization of mostly incompatible polymers is a challenge. Recent developments [13-19] showed that chain-extending cross-linkers (CECL) offer paths to improve melt strength, thermal stability and phase compatibility of polymer blends during compounding and film blowing. This may lead to tailor-made polymers for packaging applications, which is the largest market segment in the plastics industry. In Europe, 40 % of the plastics demand is used in packaging, and 50 % of all goods are packaged in plastics [20]. Thus, film blowing became the most important process in the production of polymer films [21-22]. It is important that biopolymers can be processed on PE or PP extrusion lines and adapted to any film-blowing technology for either monolayer or multi-layer films.

1.1 PBAT and PLA and their blends

1.1.1 Properties

The most promising and popular biopolymer for a wide range of applications is PBAT obtained by poly-condensation of butane diol, adipic acid, and terephthalic acid [23]. It is synthesized by a transesterification reaction. Its biodegradability results from the butylene adipate groups and its stability and mechanical properties from the terephthalate groups [24-25].

Compared to other biodegradable polyesters such as PLA and PBS (polybutylene succinate), the mechanical properties of PBAT are closer to those of LDPE, Figure 1 (left and right), making PBAT a promising biodegradable polymer for many applications. PBAT is a flexible polymer with a Young's modulus (E) of 20 to 35 MPa, a tensile strength (σ) of 25 to 40 MPa, and a high elongation at break (ε) close to 1000 % exceeding the properties of many other biodegradable polyesters such as PLA and PBS [26]. The blending of PBAT with PLA increases Young's modulus slightly but decreases the tensile strength and elongation at break [26].

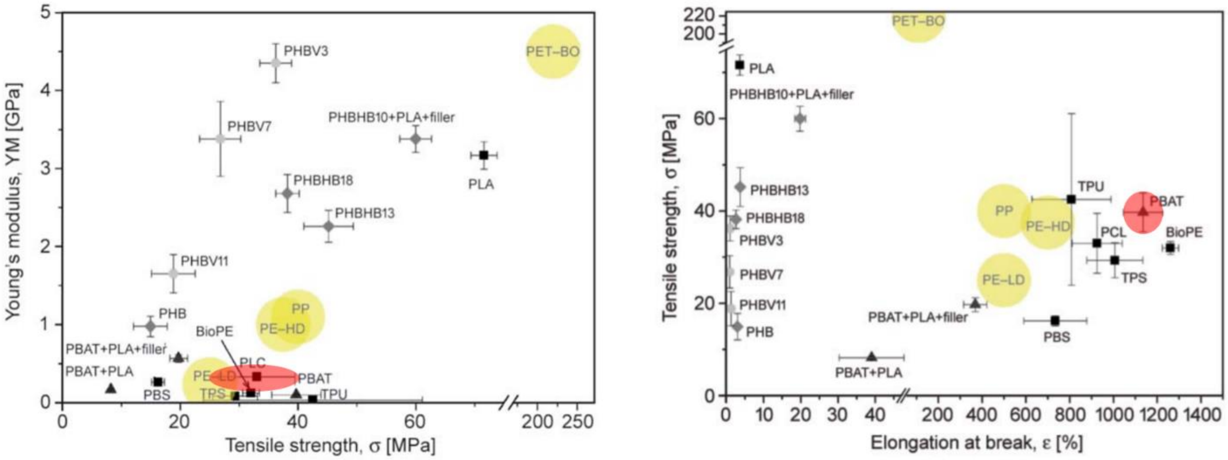

Figure 1: Plot of Young's modulus vs tensile strength for some biopolymers including PBAT (red) compared to some conventional polymers (yellow) [26] (left) and plot of tensile strength vs elongation at break for some biopolymers (right).

The performance of PBAT does not meet many customer requirements. To open new application fields, its performance has to be enhanced by blending, copolymerization, and adding fillers and modifiers. Blending with cheap polymers (e.g. starch) or reinforcing polymers (e.g. PLA) are possibilities to achieve these goals while maintaining biodegradability. PLA is produced either by ring-opening polymerization of lactides or by condensation polymerization of lactic acid monomers [27-28]. These monomers are obtained by fermentation of corn, beet-sugar, cane-sugar, etc. and have the second largest production volume of all biopolymers [8-9].

PLA is a stiff and brittle polymer with a high Young's modulus (3.4 GPa) and low elongation at break (6 %). The tensile strength (53 MPa) is similar to PET (polyethylene terephthalate) and higher compared to HIPS (high-impact polystyrene) or PP (polypropylene) [29-33]. PBAT is a candidate for toughening PLA while maintaining biodegradability, especially for extrusion film and foam applications. However, PLA and PBAT are non-compatible polymers which leads to a multiphase structure with relatively poor mechanical properties.

1.1.2 The compounding process

Compounding is the process of mixing polymers, fillers, fibers, and additives to a homogeneous polymer melt that is processable and meets the requirements of the application. In the compounding of polymer blends, selected equipment, process conditions, and blend formulation have a significant impact on the final morphology. Investigations of PBAT/PLA compounds revealed that the interfacial compatibility is poor and can be improved by introducing compatibilizers or reactive CECL [15-19].

Compounding is performed in several steps, Figure 2. The process starts with the intake of the components in a twin-screw extruder via the main hopper or side feeders. The elements of the screw are chosen to affirm fast and homogeneous mixing. The extruder temperature is chosen 20 to 30 K above the melting point of the matrix resin. Due to high temperatures and the shear stresses reactive substances such as oxygen, hydro-peroxides, and catalyst residues are created [35-37]. To control these reactions chemical agents can be added. The polymer melt exits the extruder in the form of strands of filaments having a diameter of 1 to 3 mm. After solidifying they are chopped into pellets for further use e.g. blown film extrusion.

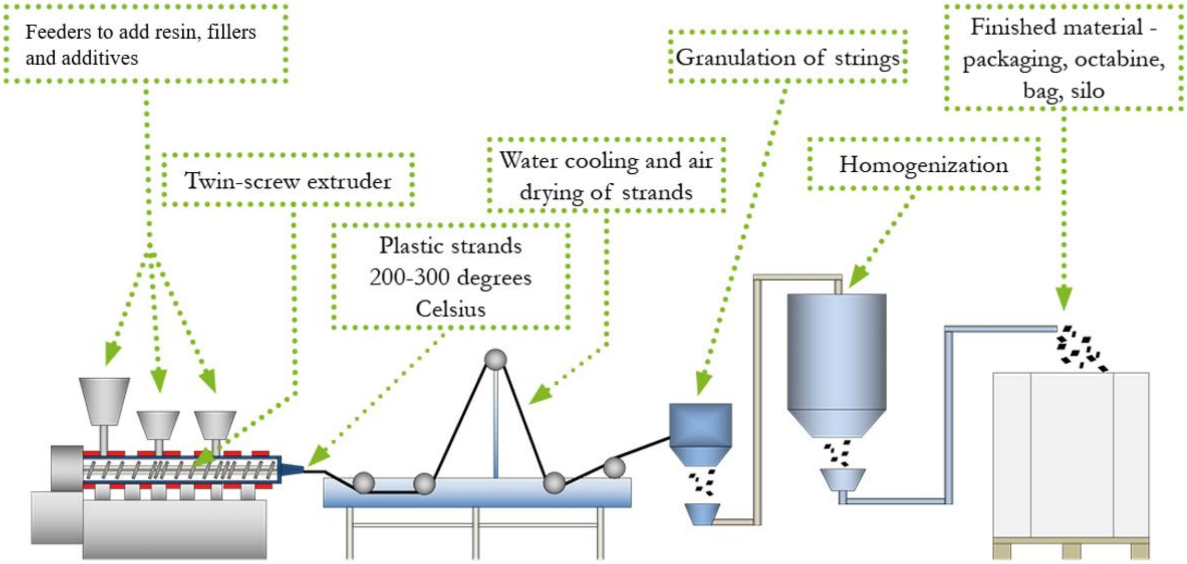

Figure 2: Scheme of the process of polymer blend compounding [34].

1.1.3 The process of blown film

Film blowing is an extrusion process to manufacture continuous polymer films mainly for packaging purposes as schematically shown in Figure 3.

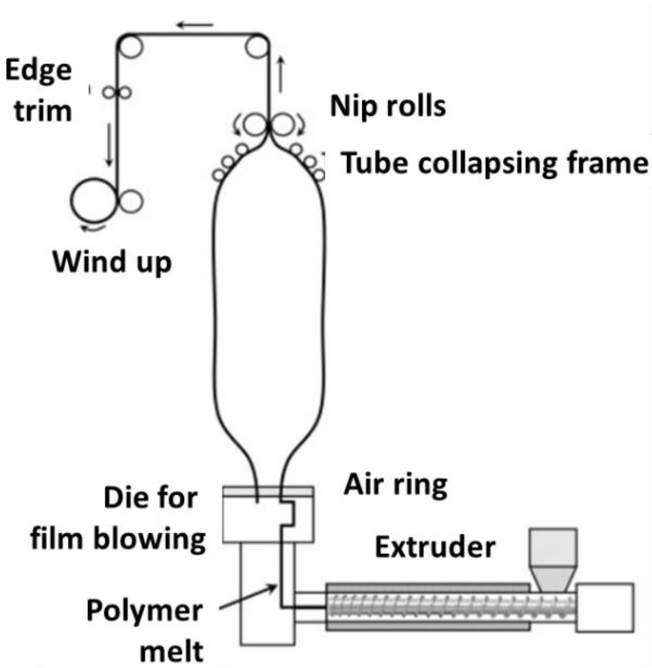

Figure 3: Scheme of a blown film process [38].

The polymer melt is extruded through a die forming a tube. This tube is vertically drawn by nip rollers and simultaneously blown and cooled by injected air through the center of the die mandrel, thus forming a tubular bubble [38-42]. Finally, this tubular bubble is flattened by nip rollers and wound up.

Relevant processing quantities are:

- **blow-up ratio (BUR)** $BUR = \frac{Bubble\ diameter}{Die\ diameter}$ (1)

- **draw ratio (DR)** $DR = \frac{thickness\ of\ ring}{BUR * thickness\ of\ film}$ (2)

During film blowing the polymer melt is drawn both in extrusion (ED) and transverse (TD) directions. This biaxial elongation orients the polymer molecules. The degree of orientation affects the film properties concerning the corresponding directions and depends on the desired film thickness determined by the thickness of the ring, BUR, and DR as well as process parameters such as melt temperature air-cooling conditions and melt viscosity [41-43]. The chosen thickness significantly affects the mechanical properties, Figures 4, 5, and 6.

The modulus of elasticity, Figure 4, in ED and TD increase with PLA content for 110 µm as well as for 25 µm thick films [42]. The tensile strength, Figure 5, in TD of 110 µm films is lower than in ED. This is attributed to the process-dependent larger melt stretching in ED compared to TD leading to a higher molecule orientation in ED.

The elongation at break, Figure 6, decreases with the increasing PLA content. This occurs for 110 µm and 25 µm films in both directions when the PLA content increases from 10 to 40 wt. %.

In general one can say that the addition of PLA to PBAT enhances elastic moduli and tensile strengths of their blends but reduces the elongations at break.

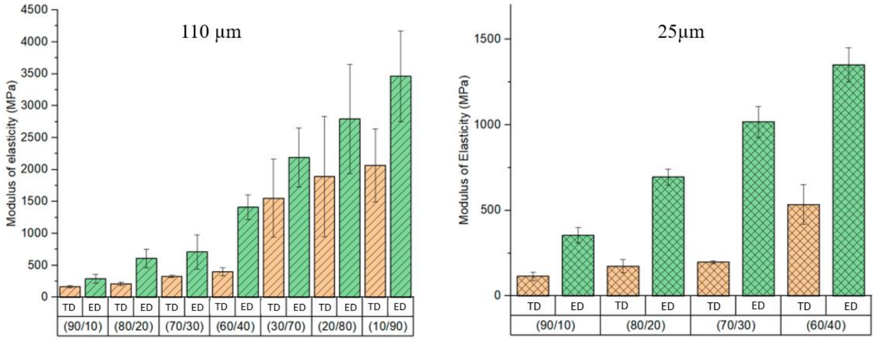

Figure 4: Elastic moduli of PBAT/PLA blends in ED and TD of 110 and 25 µm films [42].

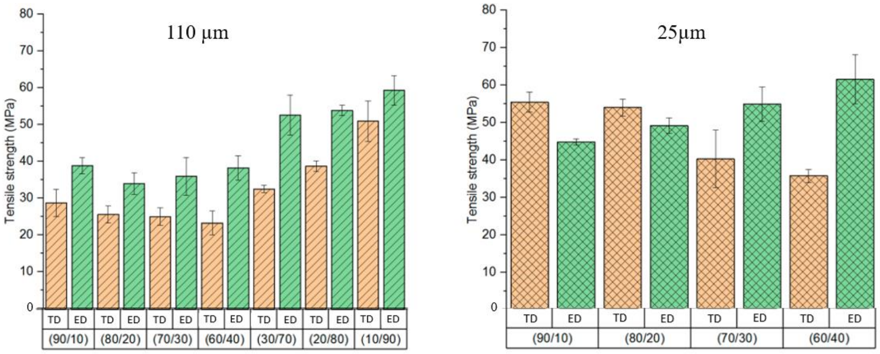

Figure 5: Tensile strengths of PBAT/PLA blends in ED and TD of 110 and 25 µm films [42].

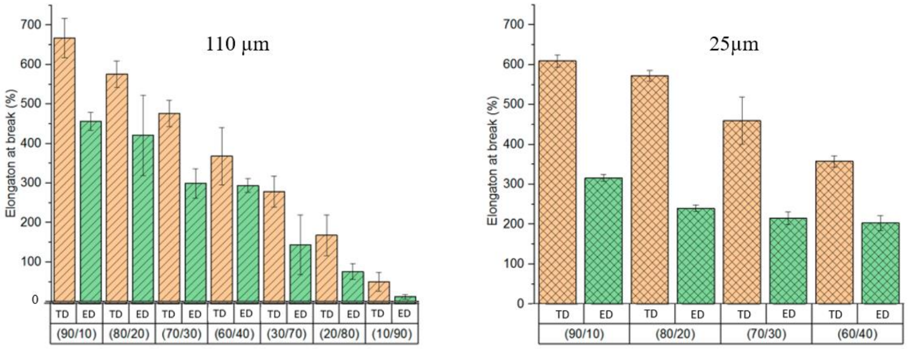

Figure 6: Elongation at break of PBAT/PLA blends in ED and TD of 110 and 25 µm films [42].

This thesis presents the innovative work of investigating the influence that blow-up ratio will have on process-induced properties and morphology, with the modification with CECL that hasn't been researched.

1.2 CECL modification of PBAT/PLA blends

Concerning the polymers related to this thesis, PBAT effectively increases the melt strength of PLA during process, but the compatibility is still insufficient due to the poor interfacial adhesion leading to thermodynamically instable morphologies and relatively weak interfacial adhesion after compounding. Thus, cross-linking is considered the most appropriate approach to overcome the limitations of these biomaterials [9,10, 13-19].

Zhou et al. [36] investigated the miscibility and crystallization behavior of PBAT/PLA blends. They found that a “chain mobility promoter” can efficaciously interact with PLA chains to develop oriented crystalline architecture, and the elongational flows can deform the dispersed PBAT phase to nano-fibrils with large surface areas. They allow for more pronounced interactions between the two phases. Dil et al. [37] studied the morphology and miscibility of PBAT/PLA blends without compatibilizer in detail and found that the diameter of the dispersed PBAT phase increased significantly. A result of partial miscibility is the continuous and co-continuous morphology development with different types of interfaces which seem to show higher interactions. These studies indicate that the level of interaction in polymer blends with low interfacial tension and their mutual miscibility/immiscibility can have a determining effect on the morphology evolution.

Al-Itry et al. [15] investigated the thermal stability of PLA and PBAT during processing and the resulting structural, rheological, mechanical and morphological properties of PBAT/PLA blends compatibilized with Joncryl® ADR 4368 (BASF). Above temperatures of 180 °C they found a decrease of molecular weight and intrinsic viscosity. The incorporation of Joncryl® increased the thermal stability, molecular weight, intrinsic viscosity, shear thinning and elasticity during processing due to the epoxy reactive functional groups.

Wang et al. [13] found that an epoxy-terminated branched polymer (ETBP) enhanced interfacial compatibility and mechanical properties. An ETBP content of 3.0 phr increased elongation at break of PBAT/PLA blends from 45 to 270 % and impact strength from 26 to 45 $\mathrm{kJm^{-2}}$. DMA measurements revealed that the difference between the T_g(PLA) and T_g(PBAT) decreased with ETBP content indicating that ETBP promotes the interfacial compatibility of PLA and PBAT phases, by proposing that the epoxy groups of ETBP reacted with the terminal carboxyl groups of PLA and/or PBAT, to enhance the interaction between the two phases.

Dong et al. [16] investigated phase morphology, mechanical properties, thermal properties and hydrolytic degradation of PLA as well as PBAT/PLA blends with and without chain extenders containing multi-epoxy groups. They improved both phase compatibility and mechanical properties. The chain-extending effect was confirmed by an increase in molecular weight. Elongations at break of PBAT/PLA blends increased from 200 % to 500 % without compromising tensile strengths.

Arruda et al. [17] investigated 60/40 % and 40/60 % PBAT/PLA blends after adding Joncryl® as CECL. Both PLA and PBAT showed improved thermal stability and increased complex viscosity. Furthermore, they found a preferential reactivity of the CECL with the PLA component. Pan et al. [18] studied melt compounded PBAT/PLA blends using MDI (4,4 methylene diphenyl diisocyanate) as CECL. Increasing MDI content led to higher yield and tensile strength, modulus and elongation at break associated with yielding deformation between the PLA and PBAT phase. Supplemented DSC, WAXS and SAXS studies suggested that amorphous PLA and PBAT can be well compatibilized with MDI due to an enhanced mobility of the amorphous phase. Therefore, crystallite dimensions are reduced in the entangled amorphous network.

1.3 Properties of modified PBAT/PLA blends after blown-film processing

The introduction of CECL to polymer blends changes their properties, which are determined by mostly standardized tests.

1.3.1 Tensile properties of modified PBAT/PLA blends

According to Arruda et al. [17] the mechanical behavior of neat PLA and neat PBAT is characterized by stress-strain curves and differs significantly, Figure 7. Furthermore, the effects of the introduction of 0.3 and 0.6 % Joncryl® can be seen. In particular, the elongation at break increased from around 400 % to 900 % for PBAT, whereas it decreased for PLA [17].

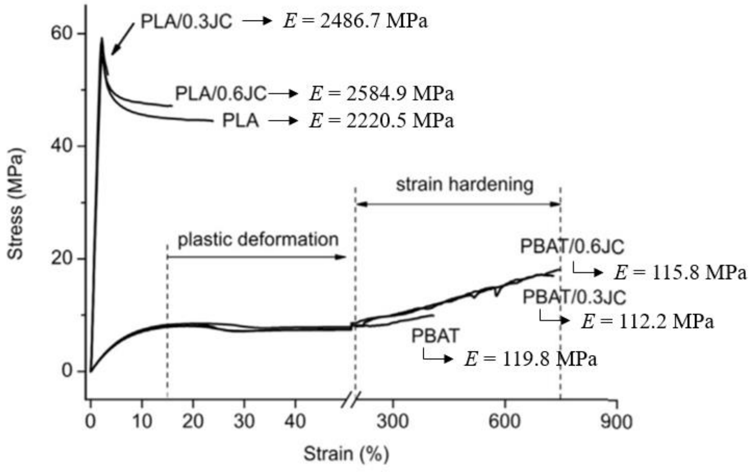

Figure 7: Stress-strain curves of neat PLA, neat PBAT and PBAT/PLA blend with different Joncryl® concentrations [17] with corresponding Young's modulus (E) values.

1.3.2 Tear properties of PBAT/PLA blends

The tear strength of blown films is a measure of their resistance against tearing forces [44-46]. Kim et al. [47] reported that blown films made by a 65/35 % PBAT/PLA blend with a thickness of 30 µm achieved an anisotropic tear resistance of 4.6 N mm^{-1} in TD and 8.7 N mm^{-1} in ED. The mixture ratio of PBAT/PLA blends has a significant effect as tear strengths increase with PBAT content, thus demonstrating that PBAT functions as an impact modifier for PLA.

Su et al. [42] have studied un-compatibilized PBAT/PLA blends with different contents of both polymers concerning tear strength properties. The tear strength increases with PBAT content, showing that PBAT functions as an impact modifier for PLA.

1.3.3 Seal strength of PBAT/PLA blends

The seal strength test is performed using a tensile testing machine that measures a force-displacement curve. The seal force is given by the plateau force and the force oscillations of the plateau contain information on the mechanisms determining seal failure.

In the sealing process, two hot jaws heat the two films to a partially molten state and press them to one another for a given time until the seal is formed [48-49]. Relevant process parameters are sealing temperature, dwell time, and pressure that affect the achievable seal strength [50]. Amorphous PLA exhibits good sealing performance with a high seal strength of 10 N as it exhibits sufficient chain mobility at the surface leading to a better inter-diffusion of molecules and adhesion under standard sealing temperatures of 140 °C. Semi-crystalline PLA is not sealable under standard sealing temperatures because this requires some melting of crystallites [51]. For economic reasons high packaging speeds are desired which require short sealing times. Therefore, it is an issue how the PBAT/PLA ratio and CECL affect the seal quality.

1.3.4 Rheological properties of modified PBAT/PLA blends

For film blowing, the polymer melt requires high melt strength [41-43]. Compared to PE, PLA and PBAT are linear polymers with rather low molecular weight, and thus, low concentration of entanglements being responsible for melt strength under elongational flow.

Chain extending and crosslinking evoke a complex rheological behavior such as the appearance of strain hardening caused by more entanglements and the formation of covalent bonds between PLA and PBAT [52]. The application of chain extenders may result in the formation of long chain branching [53].

Pure linear PLA naturally does not exhibit strain hardening [56], the PLA/PBAT blends lack this phenomenon for extension rates lower than 1 s^{-1} where the process of disentanglement prevails [54-56].

The measurement of elongational viscosity does not range to trivial operations. Ingenious devices proposed by Meissner [57-58] and Münstedt [59] in the 1980s are no longer in use. At present the field is dominated by the Sentmanat Extensional Rheometer Universal Testing Platform (SER) [57-60]. The big advantage of this apparatus is its small size enabling its housing practically in any standard rotational rheometer, where its easy manipulation makes its usage comfortable.

1.3.5 Dynamic mechanical analysis of modified PBAT/PLA blends

The characterization of thermal mechanical properties in terms of temperature dependent storage modulus *E*’ and loss modulus *E*’’ is crucial to understand the effects due to blending, mixture ratio and CECL. In Figure 8, storage moduli curves of neat PLA, neat PBAT and a 50/50 % PBAT/PLA blend are shown. Furthermore, the effects of four CECL concentrations on storage moduli of the blend are shown for MDI (4,4 methylene diphenyl diisocyanate) [18].

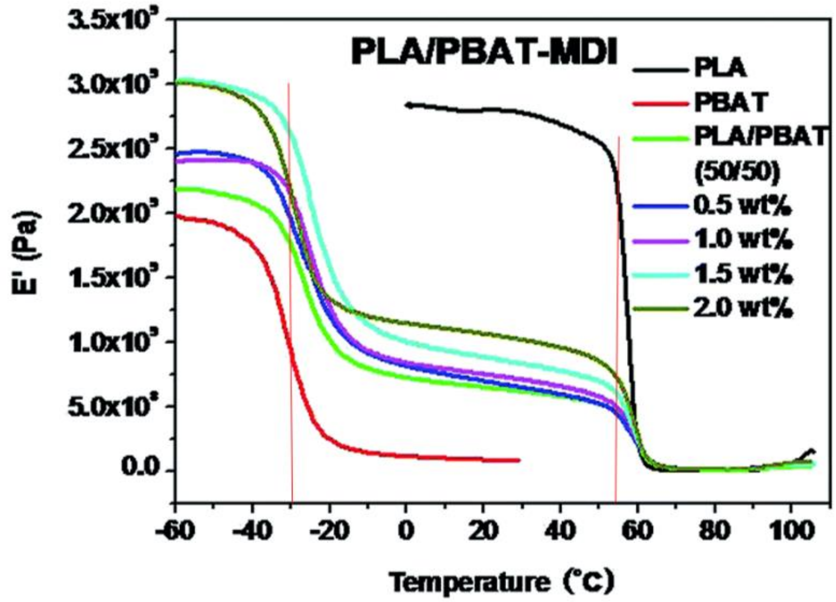

Figure 8: Temperature dependent storage moduli (E’) of PBAT, PLA and a 50/50 PBAT/PLA blend modified with CECL [18].

Dynamic mechanical analysis measurements indicate enhancement of compatibility of the PBAT/PLA-MDI blends. The pure PLA displays a high *E*’ at about 3.0 GPa, which remains in the same order up to 55 °C, while neat PBAT shows a smoother drop in *E*’ at about -30 °C. For the PBAT/PLA-MDI blends, *E*’ drops at about -30 °C, when the fraction of MDI becomes higher. This is also seen on the 50/50 % blends with the increasing of MDI percentage; the higher the amount of modifier, the higher is the shift in T_g, and also higher is the E'. The varied morphology, coupled with chemical interaction between the functional groups of the two polyesters, may affect mobility of the phases, and result in a shift of glass transition temperature with respect to the expected values [52].

1.3.6 Thermal properties of PBAT/PLA blends

As both PBAT and PLA are in principle semi-crystalline polymers, it is interesting how reactive processing affects the phase structure and, thus, the transition temperatures and corresponding enthalpies. Figure 9 shows the effects content ratio on DSC traces of PBAT/PLA blends with indication of glass and melt temperatures.

The T_g of neat PLA is around 60 °C. The T_g of PBAT is around -30 °C. The melt peak temperatures of PLA and PBAT are around 150 °C and 123 °C, respectively. T_g and T_m of PBAT/PLA blends remain at values corresponding to pure PBAT and PLA indicating a two-phase structure [53-54]. PLA shows no melting peak, and 10/90 % PBAT/PLA has pronounced crystallization and melting peaks meaning that PBAT acts as a nucleating agent. Increasing PLA content reduces the peak areas more than expected with respect to the content. At 50/50 % PBAT/PLA, crystallinity has almost vanished.

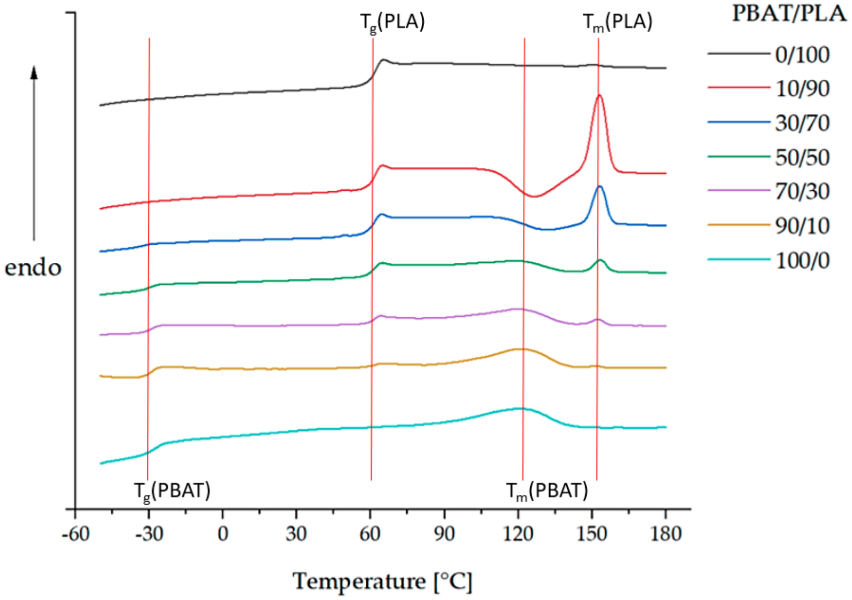

Figure 9: DSC Analysis of neat PBAT and neat PLA films [42].

IR spectroscopy may provide information of structural changes due to chemical reaction of CECL. Wu et al. [61] have investigated how Joncryl® (ADR) and dicumyl peroxide (DCP) modify the spectra of an 80/20 % PBAT/PLA blends, and found the characteristic bands at 1714 cm^{-1} for PBAT and 1752 cm^{-1} for PLA due to the –C=O stretching vibration in PBAT and PLA. The bands at 849, 908 and 1252 cm^{-1} were assigned to the –C–O stretching vibration of the ADR epoxy group.

In addition, there were no epoxy group characteristic bands in the PBAT/PLA/ADR spectra which indicate terminal carboxyl and hydroxyl groups of PLA and PBAT having reacted with the epoxy groups [15]. FTIR spectra confirmed that the epoxy group of ADR can react with the hydroxyl or carboxyl group of PLA and PBAT in reactive blending, because there were no similar epoxy group characteristic peaks in the PBAT/PLA/ADR and (PBAT/ADR)/PLA spectra which indicated the terminal carboxyl and hydroxyl groups of PLA and PBAT could react with the epoxy groups.

1.3.7 Morphological investigations of PBAT/PLA blends

1.3.7.1. Structure formation of blends

The properties of immiscible blends depend on mixture ratio of blend components and processing induced morphology. With increasing PBAT content, the equilibrium morphology of PBAT/PLA blends is changed, Figure 10 [62].

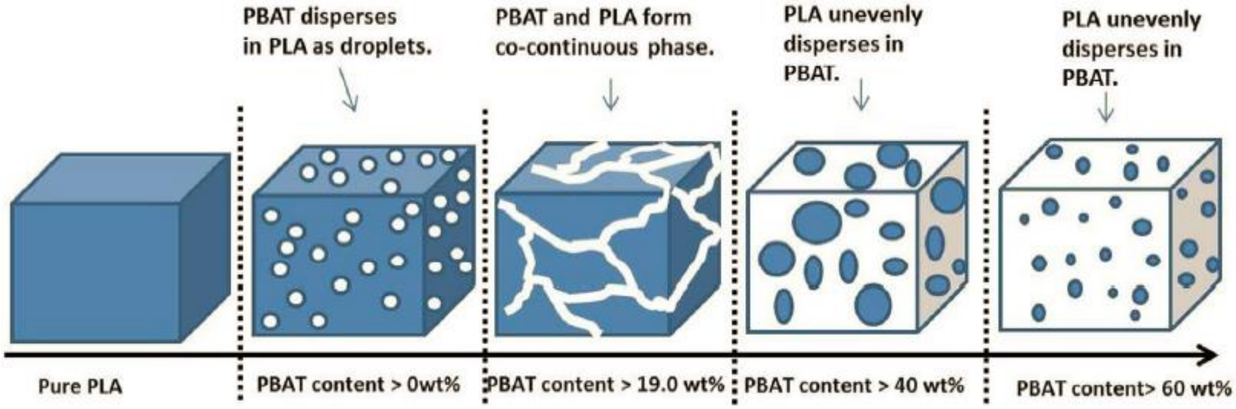

Figure 10: Schematic diagram of phase structure as a function of composition [62].

Under elongation and/or shear flow spherical droplets may deform to fibrils being solidified in that shape if rapidly cooled. The surface is more irregular with a two-phase morphology of PLA and PBAT as hard and soft phase, respectively. In liquids consisting of immiscible components the difference of surface tensions tries to minimize the surface energy of each phase. This mechanism leads to a phase structure showing spherical inclusions. Compatibilizer reduces the difference of surface tensions, and for miscible components only the external surface is left.

1.3.7.1. Processing effects on structure and properties

A few investigations deal with CECL in PBAT/PLA blends [13-17]. Fracture surfaces of films in ED and TD of 60/40 and 40/60 PBAT/PLA blends show the effects of film blowing and addition of CECL (0.3 and 0.6 % Joncryl®, respectively) [17], Figure 11. All blends exhibit a skin core structure with smaller dimensions of the dispersed phase closer to skin than in core. This is attributed to the fact that close to the skin the dispersed phase is stretched to longer and thinner fibrils, which then decay to smaller droplets. Furthermore, the polymer melt is colder than in the core, thus, having a higher melt viscosity avoiding relaxation to coarser structures of the dispersed phase.

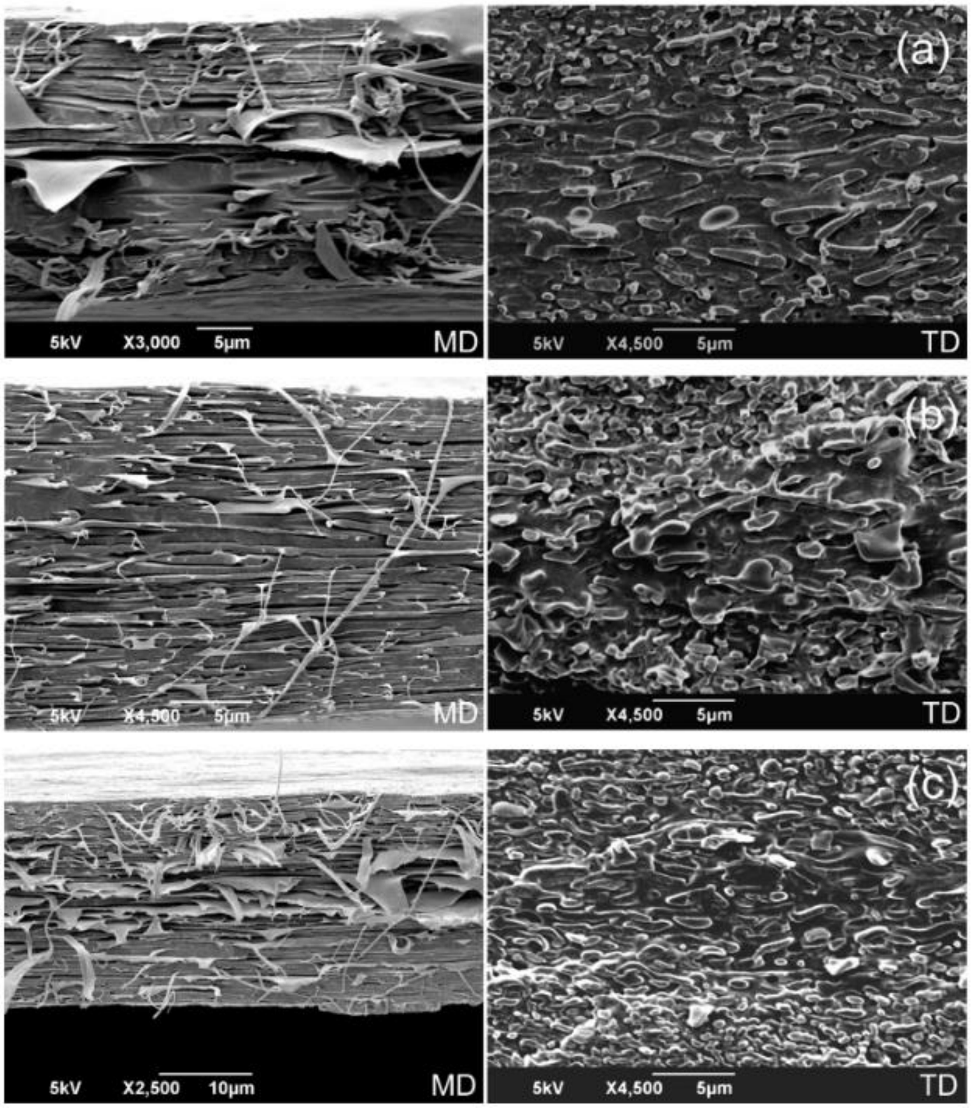

Figure 11: Fracture surface of a PBAT/PLA 40/60 % blend in SEM in ED and TD - (a) without CECL, (b) with CECL 0.3 % Joncryl®, (c) with CECL 0.6 % Joncryl® [17].

The fracture surfaces of the 40/60 % PBAT/PLA blends, Figure 11, show that the dispersed phase is elongated to fibrils with aspect ratios exceeding 5 in ED due to a high DR, whereas it is deformed to ellipsoids in TD with aspect ratios between 2 and 4. With increasing CECL content the aspect ratios become smaller indicating that the reactions of CECL have increased the melt viscosity. The dispersed phase cannot be oriented furthermore. Without CECL, the fracture surfaces exhibit a brittle character that seems to become slightly more ductile by adding CECL. Both the reduced aspect ratios of the dispersed phases, and the slightly increased ductility show that CECL additions below 1 % are a tool to adjust properties of PBAT/PLA blends.

1.4 Disintegration process of PBAT/PLA blends

The advantage of biodegradable polymers is that they "vanish" if they are exposed to environmental conditions after becoming waste. One distinguishes different environmental conditions (compost, soil, water, different temperatures and under aerobic or anaerobic influences) under which biopolymers may degrade. According to the IUPAC[1] definitions, biodegradation means degradation caused by enzymatic processes resulting from the action of living cells [63-65]. Lucas et al. [63] classified the process in three main steps:

- **biodeterioration** is materials fragmentation in tiny pieces due to decomposers such as microorganisms and/or abiotic factors;
- **depolymerization and biofragmentation** is molecular mass reduction due to chain cleavages;
- **mineralization and biomass production** mean uptake of small molecules into the living cells and therein conversion to biomass, storage vesicles and metabolites. This finally leads to total mineralization, which is the formation of simple molecules such as H_2O and CO_2.

For polyesters, such as PLA, PBAT and their blends, hydrolysis either purely chemical or enzymatic mediated is a dominantly occurring process [65-68]. Tolga et al. [66] have studied the time dependent disintegration processes of three biopolymer blends under industrial composting conditions. They found that degradation started after an incubation time of 5 to 6 weeks, whereas the two PBS/PLA blends started after 4 weeks. After an incubation period in which PLA is subjected to hydrolytic degradation until the polymer segment have reached a length enabling microorganisms to attach. This step is characterized by a slight weight increase due to water absorption. In the next step, microorganisms will deteriorate the segments and produce biomass, water and CO_2. Once started, hydrolytic degradation in PLA proceeds faster in the inner molecular structure than on the outer surface due to the fact that water penetrates the material and generates chain cleavages in amorphous regions at the ester bonds. Once initiated, the process accelerates as a consequence of a high amount of carboxylic end groups being formed, which decreases the pH in the inner core of the PLA material. Additionally, an erosion process on the specimen's surfaces in the present biotic environment accelerated by enzymatic action is also to be expected as being already shown in the literature [67-68].

---

[1] *IUPAC - International Union of Pure and Applied Chemistry*

2. AIM OF THE WORK

The global plastic waste problems positively affected the development of biopolymers and other sustainable materials leading to the substitution of traditional packaging plastics with biodegradable polymers. However, for more demanding engineering applications, their mechanical properties must be enhanced without compromising their biodegradability. Many biopolymers are combined with other polymers to balance the properties required for specific applications. Compounding is used to make a biopolymer fit for specific applications by blending it with other polyesters and adding chain extenders cross-linkers to provide optimized properties.

Currently little is known about how multi-functional chain extenders cross-linkers (CECL) affect the properties and morphologies of PBAT-PLA blends. Therefore, the objective of this study is to investigate the effects of four CECLs on the morphology of PBAT-PLA compounds to optimize processability and usage performance.

The largest market in the plastics industry is the packaging segment with more than 40 % of plastics demand in Europe. Blown film extrusion is the most important industrial manufacturing process of polymeric films.

As for all polymer processing techniques, blown film processing parameters e.g. extrusion temperature, blow-up ratio, and draw ratio affect the thermo-viscoelastic properties and the morphological structure of the film, have been collected. Within this work, the process-induced thermo-viscoelastic and mechanical performance is to be investigated using dynamic mechanical analysis, tensile properties, and differential scanning calorimetry. To further obtain a better insight, the morphological structure will be examined by scanning electron microscopy and elongational rheology. Moreover, the impact of the biodegradation (disintegration effect) is also studied to see which effect CECL can have on the rate of disintegration in blown films.

The morphologies are interpreted concerning structure formation during film blowing with a blow-up ratio and a draw ratio, where the temperature and CECL are dependent on melt viscosities of blends of PBAT and PLA. After extrusion, elongation flows stretch and orient the melt, at the beginning in the transverse direction, due to blowing, and subsequently in the extrusion direction, due to the drawing. Rate-dependent shear and elongation viscosity measurements would provide a deeper understanding of the effects that the introduced CECL has on melt viscosities and the process-generated film morphologies.

The presented results are also summarized in the following publications:

I **The Effects of Chain-Extending Cross-Linkers on the Mechanical and Thermal Properties of Poly(butylene adipate terephthalate)/Poly(lactic acid) Blown Films.**
J. V. C. Azevedo, E. R. Dorp, B. Hausnerová, B. Möginger;
Polymers, 2021, Volume 13, 3092.
Paper I

II **Process-induced morphology of poly(butylene adipate terephthalate)/poly(lactic acid) blown extrusion films modified with chain-extending cross-linkers.**
J. V. C. Azevedo, E. R. Dorp, R. Grimmig, B. Hausnerová, B. Möginger;
Polymers, 2022, Volume 14, 1939.
Paper II

III **Effect of Chain Extending Cross-Linkers on the Disintegration Behavior of Composted PBAT/PLA Blown Films.**
J. V. C. Azevedo, B. Hausnerová, B. Möginger, T. Šopík;
International Journal of Molecular Sciences, 2023, Volume 25(5), 4525.
Paper III

IV **Improvement of elongational behavior of poly(lactic acid)/poly(butylene adipate terephthalate) blends in blown film extrusion using chain extending cross-linkers.**
P. Filip, B. Hausnerová, B. Möginger, J. V. C. Azevedo;
Submitted to *International Journal of Biological Macromolecules*, November 2023
Paper IV

V **Blow molding-induced structure and performance of renewable PLA/PBAT packaging films modified with chain-extending cross-linkers.**
J. V. C. Azevedo, E. R. Dorp, C. Kössler, C. Thomser, T. Šopík, B. Möginger B. Hausnerová;
Submitted to *Journal of Industrial and Engineering Chemistry*, November 2023
Paper V

A better understanding of the introduction of the CECLs in PBAT PLA blends provided in the thesis, Figure 12, will lead to predictions of the CECL effects on blown film extrusion and film properties.

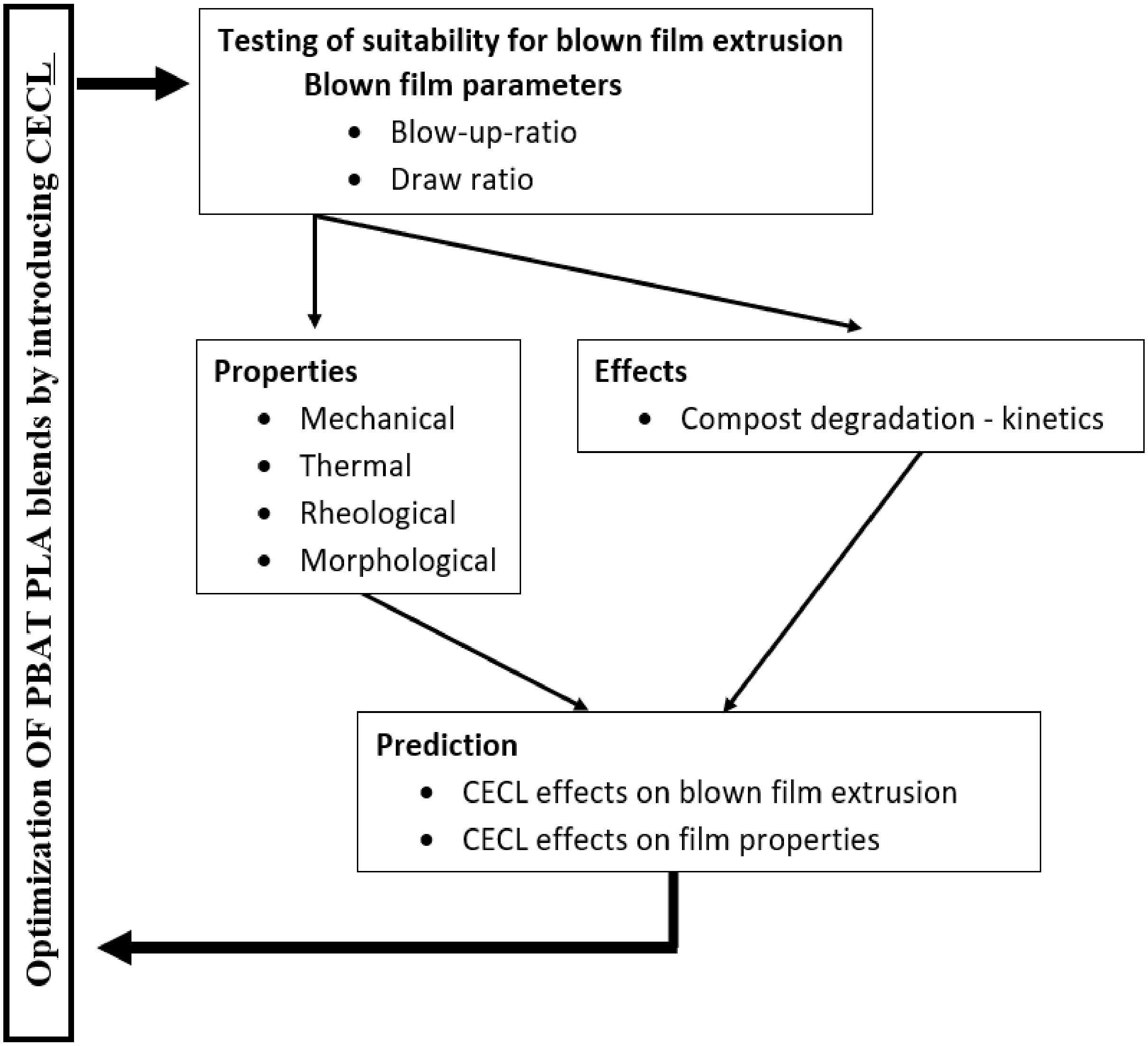

Figure 12: Flow chart of the methodology and techniques employed in this PhD thesis.

3. MATERIALS AND METHODS

Four CECL (1 wt. %), Table 1, were compounded into the reference PBAT-PLA (REF) compound named M·VERA® B5029 [69] from BIO-FED, a branch of AKRO-PLASTIC GmbH, Germany developed before this dissertation, and which is now used for packaging (fruit and vegetable bags, labels) and agricultural applications:

Table 1 Information about the CECL used with the introduction of chemical name, trade name and manufacturer.

	Chemical name	Trade name	Manufacturer
V1	tris(2,4-di-tert-butylphenyl)phosphite	Songnox™ 1680	Songwon Industrial Co [70]
V2	1,3-phenylenebisoxazoline	1,3-PBO powder	Evonik [71]
V3	aromatic polycarbodiimide	Stabaxol® P110	Lanxess [72]
V4	poly(4,4-dicyclohexylmethanecarbodiimide)	Carbodilite™ HMV-15CA	Nisshinbo [73]

All ingredients were uniformly mixed using a Mixaco CM 150-D (Mixaco Maschinenbau, Germany) and compounded in a twin-screw extruder (FEL 26 MTS, Feddem GmbH, Germany) with a diameter of 32 mm and a L/D of 26, screw speed of 260 rpm and output rate of 20 kg h^{-1}. The films were blown using an LF-400 (Labtech Engineering Company, Thailand) machine with a single screw having a diameter of 25 mm and an L/D of 30, extrusion temperature of 165 °C, and blow-up-ratio (BUR) of 1:2.5 for both 25 µm and 100 µm films. From an extrusion gap of 0.8 mm, the draw ratio was estimated from 12 to 14 for 25 µm films and 3 to 4 for 100 µm films. The extrusion pressures were 240 bar for the REF blend, 290 bar (V1), 159 bar (V2), 230 bar (V4) and 313 bar (V4). Before testing, all films were stored for 24 h at 23 °C/50 % r.h. Further films with different BUR were made and on Table 2 is presented the thickness with standard deviation (STD) and draw ratio (DR).

Table 2 Mean thicknesses of films of REF, V1 to V4 with the following standard deviation (STD), blow-up ratio (BUR) and draw-ratio (DR).

	BUR 1.5			**BUR 2.5**			**BUR 3.5**		
	Thickness (µm)	STD	DR	Thickness (µm)	STD	DR	Thickness (µm)	STD	DR
REF	26.0	1.0	20.5	25.8	0.7	12.4	26.0	1.0	8.8
V1	27.0	1.0	19.8	30.5	0.5	10.5	26.4	0.5	8.7

V2	26.6	0.9	20.1	26.3	0.5	12.2	26.0	0.7	8.8
V3	27.4	0.5	19.5	27.3	0.6	11.7	26.6	0.5	8.6
V4	25.2	0.4	21.2	29.9	0.8	10.7	26.2	0.4	8.7

The introduction of CECL to polymer blends changes their properties, which are determined by mostly standardized tests summarized in Table 3.

Table 3 Standardized tests for the studied REF and respective blends.

Test procedure	**Standard**	**Instrument**	**Determined properties**
Tensile test	ISO 527-3	2.5 kN Zwicki Roell	Young's modulus E Tensile strength σ_{max} Strain at break ε_{break}
Tear test	ISO 6383-2	Elmendorf teat Maschine	Rupture force F_{break} Tear resistance F_{tear}
Seal strength test	DIN 55529	2.5 kN Zwicki Roell	Seal strength F_{seal}
Gel permeation chromatography (GPC)		Waters model e2695 and Waters model 2414 differential refractometer	Number molecular mass M_n, Weight molecular mass M_w
Sentmanat Extensional Rheometer (SER).		SER Universal Testing Platform (model SER-HV-P01)	Elongational rheology
Dynamic mechanical analysis (DMA)	-	Netzsch DMA 242 E *Artemis*	Storage modulus E' Loss modulus E''
Dynamic scanning calorimetry (DSC)	ISO 11357-3:2018	Netzsch DSC 214 Polyma	Glass temperature T_g Melting temperature T_m Melting enthalpy ΔH_m Crystallization temperature T_{cr}

			Crystallization enthalpy ΔH_{cr}
IR spectroscopy (FT-IR)	-	Perkin Elmer Spectrum Spotlight 200	-
Scanning electron microscopy (SEM)	-	JSM-7200F	-
Disintegration	ISO 16929:2018		Disintegration rate Mass changes
Melt Volume Rate (MVR)	ISO 1133	Göttfert MI-3	MVR (190°C, 2,16kg)

4. Discussion of the Results

4.1 Behavior under deformation

4.1.1 Mechanical properties

Processing influences material structure and properties. Due to the blown film processing, the mechanical properties are anisotropic. In order to evaluate the effect of chain-extenders cross-linkers (CECL) on the process-induced mechanical properties relationship, Young's modulus E, tensile strength σ_{max}, elongation at break $\varepsilon_{\text{break}}$, tear resistance F_{tear} in extrusion direction (ED) and transverse direction (TD) and seal strength F_{seal} as well as the melt volume rate (MVR) were determined. Tests were performed on the unmodified blend (REF) after conditioning for 24 hours for stabilizing (initial) and after thermal aging for 1 and 2 months at 50 °C, Table 4.

Initial E and F_{tear} in ED clearly show higher values than in TD, whereas the elongation at break coincides with standard deviations (STD). This can be explained by the molecular orientation in ED caused by film blowing resulting in a flow-induced stiffening [74]. Furthermore, melt volume rate (MVR) increases by 20 % and 40 % after 1 and 2 months, respectively. This reduction of the mechanical properties and the increase in flowability after thermal aging indicates chain scission or degradation of polymer chains.

Table 4 Mechanical properties and MVR of unmodified REF blend in extrusion direction (ED) and transverse direction (TD): initial and aged for 1 and 2 months at 50 °C. (Paper I)

Property	Initial	1 month	2 months
E_{ED} (MPa)	457±36	437±37	363±48
E_{TD} (MPa)	181±22	238±10	197±12
$\sigma_{\text{max, ED}}$ (MPa)	27.8±3.1	20.4±2.6	21.2±1.5
$\sigma_{\text{max, TD}}$ (MPa)	28.8±3.1	21.8±2.2	26.1±1.8
$\varepsilon_{\text{break, ED}}$ (%)	400±48	310±39	410±26
$\varepsilon_{\text{break, TD}}$ (%)	450±27	390±20	500±20
$F_{\text{tear, ED}}$ (N mm^{-1})	107±3	104±33	80±25
$F_{\text{tear, TD}}$ (N mm^{-1})	54±17	57±18	51±16
F_{seal} (N mm^{-1})	7.0±0.3	5.9±0.4	4.8±0.6
MVR (cm^3 10 min^{-1})	4.0±0.1	4.7±0.1	5.5±0.2

Table 5 shows the properties of introducing the CECL V1 to V4. While E of V1 to V3 show only slight differences compared to the initial, V4 shows a clear increase of up to 40 % in both ED and TD. Additionally, σ_{max}, ED and TD, for V1 and V4 show only a slight increase, and σ_{max} for V2 and V3 show only a slight decrease, whereas the $\varepsilon_{\text{break,ED}}$ reveals a clear decrease in ED with similar values in TD. This can be explained by the combination of the effect of various CECLs and the increasing orientation causing a stiffening effect during tensile testing.

The tear resistance only shows a minor increase in ED and a little decrease in TD. Furthermore, the seal strength for V1 decreases dramatically, whereas for V2 to V4, it depicts a relevant increase.

Thermal aging reveals an increase of up to 25 % for E for V4 in ED after 2 months, while for the rest of the blends, it remains constant. σ_{max} increases for V2 in ED and TD after 1 month. Furthermore, $\varepsilon_{\text{break}}$ in ED decreased up to 40 % for V3 and V4 after 1 month and up to 50 % for V1 to V4 after 2 months. This is explained by the fact that thermal aging causes hydrolysis of the macromolecules prompting a pronounced effect of further degradation of the polymer chains in the blends.

This is also in line with the decreasing F_{tear} in the TD, especially after 2 months. The seal strengths decreased for V1, V3, and V4 to close to “zero”, indicating a complete loss of the sealing capability after 2 months. Only V2 showed an increase in the seal strength in the range of 10 to 25 %. The importance of seal strength is of huge interest to the packaging industry since the content needs to be restrained inside the bag. Here the stretching and deformation caused by the application load is distributed directly on the seal area and therefore needs to be minimized. Therefore, a decrease of F_{seal} after aging has a negative impact on packaging.

MVR measurements show a clear increase for V1 and V2, which demonstrates chain scission or degradation of polymer chains. On the contrary, the MVR of V3 and V4 decreases up to 80 %, indicating a cross-linking effect.

Table 5 Mechanical properties and MVR of modified compounds V1 to V4 in extrusion direction (ED) and transverse direction (TD) aged for 1 and 2 months at 50 °C. (Paper I)

	Initial				
Prop.	**REF**	**V1**	**V2**	**V3**	**V4**
E_{ED} (MPa)	457±36	399±42	501±31	407±66	627±56
E_{TD} (MPa)	181±22	177±22	162±45	147±5	380±66
$\sigma_{\text{max, ED}}$ (MPa)	27.8±3.1	31±3	24±2	22±3	33±3
$\sigma_{\text{max, TD}}$ (MPa)	28.8±3.1	33±3	24±2	25±2	35±3
$\varepsilon_{\text{break, ED}}$ (%)	400±48	210±10	250±31	250±31	240±14
$\varepsilon_{\text{break, TD}}$ (%)	450±27	450±30	450±30	460±16	440±27
$F_{\text{tear, ED}}$ (N mm^{-1})	107±3	123±38	110±34	118±38	112±35
$F_{\text{tear, TD}}$ (N mm^{-1})	54±17	41±13	35±11	40±13	40±12

F_{seal} (N mm^{-1})	7.0±0.3	0.4±0.2	8.5±0.3	8±0.6	10±2
MVR (cm^3 10 min^{-1})	4.0±0.1	5.0±0.1	5.8±0.2	0.6±0.1	1.0±0.1
	Aging 1 month at 50 °C				
Prop.	**REF**	**V1**	**V2**	**V3**	**V4**
E_{ED} (MPa)	437±37	379±21	422±20	453±16	454±38
E_{TD} (MPa)	238±10	183±10	182±18	206±11	265±33
$\sigma_{max, ED}$ (MPa)	20.4±2.6	20±1	22±2	31±1	30±1
$\sigma_{max, TD}$ (MPa)	21.8±2.2	22±2	23±2	33±2	31±1
$\varepsilon_{break, ED}$ (%)	310±39	270±17	260±17	200±16	220±11
$\varepsilon_{break, TD}$ (%)	390±20	450±23	480±15	450±32	420±19
$F_{tear, ED}$ (N mm^{-1})	104±33	139±43	142±44	132±41	111±35
$F_{tear, TD}$ (N mm^{-1})	57±18	35±11	31±10	30±10	29±9
F_{seal} (N mm^{-1})	5.9±0.4	0.4±0.2	6.5±0.3	0.6±0.1	0.9±0.1
MVR (cm^3 10 min^{-1})	4.7±0.1	5.5±0.2	6.3±0.2	0.4±0.1	1.4±0.1
	Aging 2 months at 50 °C				
Prop.	**REF**	**V1**	**V2**	**V3**	**V4**
E_{ED} (MPa)	363±48	400±11	436±26	436±37	460±27
E_{TD} (MPa)	197±12	187±23	207±20	207±14	236±25
$\sigma_{max, ED}$ (MPa)	21.2±1.5	20±2	32±2	32±3	30±2
$\sigma_{max, TD}$ (MPa)	26.5±1.8	21±1	36±2	36±3	29±3
$\varepsilon_{break, ED}$ (%)	410±26	250±24	200±20	200±32	210±10
$\varepsilon_{break, TD}$ (%)	500±20	430±14	480±39	480±29	430±33
$F_{tear, ED}$ (N mm^{-1})	80±25	138±43	130±30	112±35	109±34
$F_{tear, TD}$ (N mm^{-1})	51±16	31±13	32±11	30±10	43±14
F_{seal} (N mm^{-1})	4.8±0.6	0.6±0.3	5.5±0.9	0.5±0.1	-
MVR (cm^3 10 min^{-1})	5.5±0.2	5.9±0.2	7.9±0.3	0.35±0.1	1.2±0.1

These results show that the considered CECLs influence on both mechanical properties and flowability, also affected by aging time and temperature. From these results, it is possible to deduce that the introduction of the CECL V1 and V2 leads to chain scission or polymer chain degradation, whereas V3 and V4 indicate a cross-linking effect.

Gel permeation chromatography (GPC) was performed to evaluate if molecular degradation has occurred, Table 6. The results confirm the earlier findings of MVR measurements that the CECL causes cross-linking in V3 and V4 as their molecular masses ($M_n \approx 75{,}000$ g/mol) are roughly doubled compared to REF. REF, V1 and V2 with molecular masses around 44,000 g/mol showed that the CECL did not significantly change the molecular masses and as a consequence the macromolecular structure. Most CECL molecules have to remain as low molecular components in the polymer chain scission. The significantly higher MVR values of V1 and V2 compared to REF were explained by chain scission. However, according to the GPC results, Table 6, this cannot be the reason for the higher MVR values. They have to be explained by an enhancement of the melt flowability provided the remaining unreacted CECL as low molecular components.

Table 6 Determination of the mean molecular masses due to GPC measurements with number-average molecular mass M_n, weight-average molecular mass M_w, and polydispersity index of the polymer PDI; accuracy of measurements is 2,000 g/mol for M_n and 3,000 g/mol for M_w. (Paper III)

Compound	M_n	M_w	**PDI**
	g/mol	g/mol	-
	Initial state		
PBAT	43,000	107,000	2.45
REF	44,000	83,000	1.89
V1	42,000	81,000	1.92
V2	46,000	92,000	1.98
V3	75,000	149,000	1.99
V4	72,000	141, 000	1.95
PLA	218,000	309, 000	1.42

Due to the film-blowing process with different BUR and DR in ED and TD, anisotropic mechanical behavior and corresponding differences in a morphological structure can be expected. Figure 13 a-d shows Young's modulus E for the various BUR (1.5, 2.5 and 3.5), the tensile strength $\sigma_{\max}$, the elongation at break ε_{break} and the tear resistance F_{tear} in the ED and TD. The different BUR and the film morphology strongly influenced the mechanical properties. For a BUR of 1:2.5, the introduction of CECL modified the properties of the REF.

The E, Figure 13a, with increasing BUR, E decreases in ED. As the film is stretched in ED the structure deforms into an iso-stress pattern, where E is dominated by the amorphous phase. In TD however, E increases for V1 to V4 and slightly decreases for REF, showing that when stretching takes place in TD, the structure deforms in an iso-strain pattern and the E is dominated by the crystalline phase.

Continuing the comparison BUR 1.5 to 3.5, the results show that with increasing BUR the $\sigma_{\max}$ in ED slightly decreases, for REF, V2 and V3, but for V1 a more distinct decrease was measured, Figure 13b.

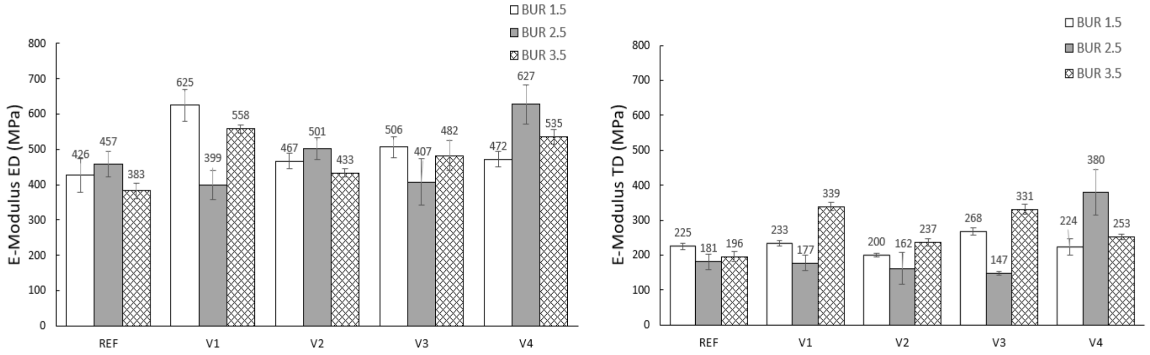

Figure 13a: Young's modulus E for REF and V1 to V2 with the different BUR: 1.5, 2.5 and 3.5, in ED and TD directions. (Paper V)

In TD however, $\sigma_{\max}$ increases with increasing BUR (1.5 vs 3.5) for all blends. Increasing the BUR causes an increase of molecular orientation in TD and a decrease in orientation in ED due to a higher feed rate to maintain constant thickness.

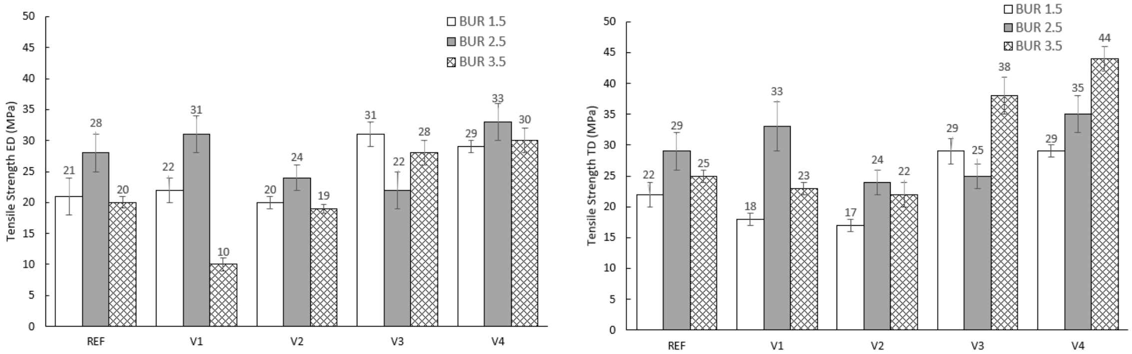

Figure 13b: Tensile strength σ_{max} for REF and V1 to V2 with the different BUR: 1.5, 2.5 and 3.5, in ED and TD directions. (Paper V)

Concerning $\varepsilon_{\text{break}}$, Figure 13c, in ED the values increase from lower BUR to higher BUR, and in TD it decreases from BUR 1.5 to 3.5. The higher surface area to cool the bubble at higher BUR could be a major factor in the lower crystallinity, resulting in a higher TD elongation. Thus, the non-uniform stretching behavior reflects the anisotropic orientation of the blends.

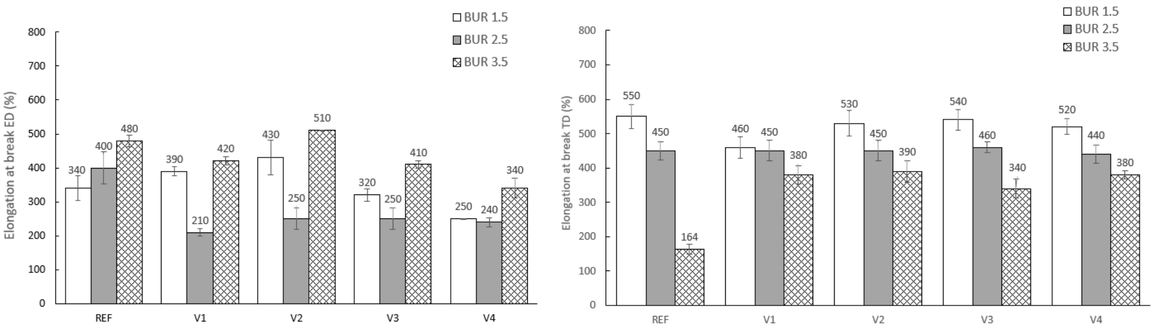

Figure 13c: Elongation at break ε_{break} for REF and V1 to V2 with the different BUR: 1.5, 2.5 and 3.5, in ED and TD directions. (Paper V)

Regarding the tear resistance, Figure 13d, in ED a decrease from BUR 1.5 to 3.5 for REF, V1 and V4 while for V2 and V3 an increase was measured. First, the decrease can be explained by the nucleated structure where a high degree of chain orientation along ED leads to poor tear strength in that direction. This is due to the fact that the tear propagation parallel to the backbone chain requires less energy than propagation perpendicular to the backbone chain. For the increase in V2 and V3, as evidenced already, the cross-linking effect could lead to higher energies being promoted for the propagation into the backbone chain. In TD, the decrease reaches more than 50 % from BUR 1.5 to 3.5, where films are unable to resist tear propagation along TD for BUR 3.5.

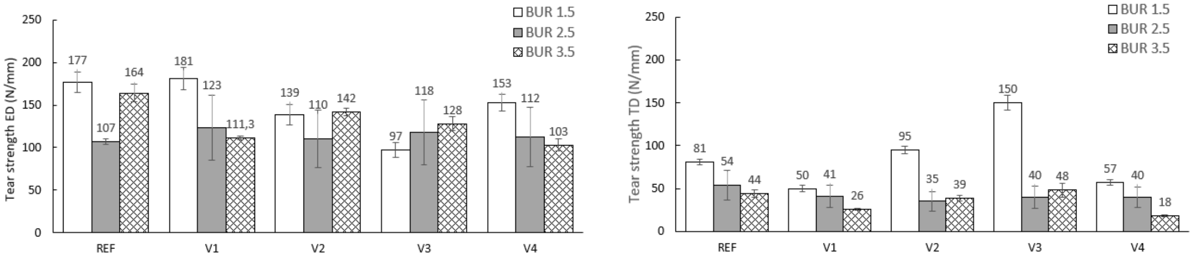

Figure 13d: Tear resistance F_{tear} for REF and V1 to V2 with the different BUR: 1.5, 2.5 and 3.5, in ED and TD directions. (Paper V)

Seal strength behavior, Figure 14, shows relatively constant values for the various BURs. Except for V2 and V4, BUR 2.5 a clear increase of 25 % was measured compared to REF, indicating that independently of the BUR, V2 and V4 characteristics of cross-linking are shown as reported above.

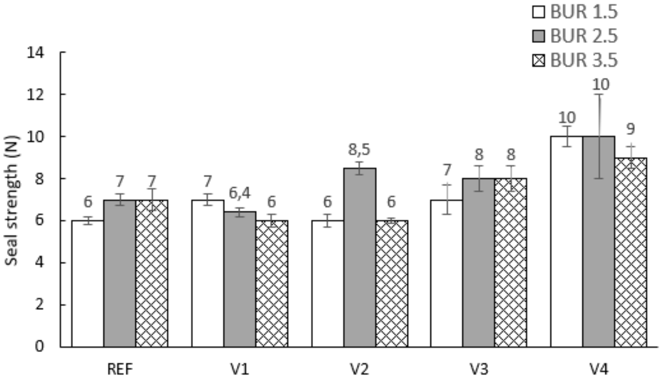

Figure 14: Seal strength for REF and V1 to V2 with the different BUR: 1.5, 2.5 and 3.5, in ED direction. (Paper V)

Summarizing it, small BUR corresponding to large DR, the macromolecules of the melt are highly oriented in ED easing crystallization in relatively thick lamellae that grow in TD. These lamellae may fix the highly oriented amorphous regions. Thus, the macromolecules of the rubbery amorphous PBAT phase keep their orientation states and increase stiffnesses in ED and decrease elongations at break in ED compared to TD. As the crystallinity of PBAT is around 15 %, the lamellae represent "solid platelets" in between oriented macro-molecules of the amorphous phase are sheared. This explains the roughly 50 % reduction of stiffnesses in TD compared to ED and the larger elongations at break.

With increasing BUR, the orientation of the macromolecules is increased in TD and decreased in ED causing inclined preferential orientations with respect to ED. Because of the biaxial orientation of the macromolecules, thinner crystalline lamellae grow with an inclination preferentially in TD and between them, thin and short cross-lamellae grow preferentially in ED, Figure 30 right. The orientation in ED still exceeds that in TD significantly even at BUR=3.5. Thus, one expects increasing elongations at break in ED – true if one compares BUR=1.5 and BUR=3.5 but not for V1 to V4 at BUR=2.5 – and decreasing elongations at break in TD – true for REF, V1 to V4 at all BUR.

With the BUR evaluation, the tensile strengths do not depend systematically on BUR. This concludes that the different processing induced BUR dependent lamellae structures have only minor effects on tensile strengths and that the tensile strengths are mainly determined by the entanglement density in the PBAT phase. This explains the higher tensile strengths V3 and V4 both in ED and TD with double molecular masses compared to REF, V1 and V2.

4.1.2 Viscoelastic properties

Both CECL compounding and processing affect temperature-dependent storage moduli in ED and TD in terms of T_g shifts and changes in stiffness. Viscoelastic properties were measured on 100 µm films because the resolution of the DMA was insufficient for the 25 µm films.

Figure 15 shows the comparison of temperature-dependent logarithmic storage moduli of REF and V1 to V4 in ED and TD at 1 Hz. For both ED and TD, T_g of the soft segment ($T_{g,ss}$) can be detected around -40 °C and for the hard segment ($T_{g,hs}$) around 50 °C. E' between $T_{g,ss}$ and $T_{g,hs}$ increase in ED for V1 and V4 compared to REF. Although, V2 and V3 show lower E' values than REF at lower temperatures, but don't differ between $T_{g,ss}$ and $T_{g,hs}$. Above $T_{g,hs}$ only V1 shows similar values as REF, while V2 to V4 present lower stiffness. In TD, V1 exhibits an increase in storage modulus, whereas only slight increases are observed for V2, V3 and V4 compared to the REF. Analogous to ED, above $T_{g,hs}$ only V1 depicts higher stiffness and V2 to V4 clearly shows lower stiffness. Overall, the moduli increase is more pronounced in ED compared to TD, which presents anisotropic behaviour. This shows that CECL reactions are leading to cross-linking for V1 and V4, whereas the shift of the $T_{g,hs}$ to lower temperatures indicates chain scission or degradation.

Meanwhile, V2 and V3 hardly show any differences in stiffness but above $T_{g,hs}$ both depict lower values which indicates chain scission or degradation.

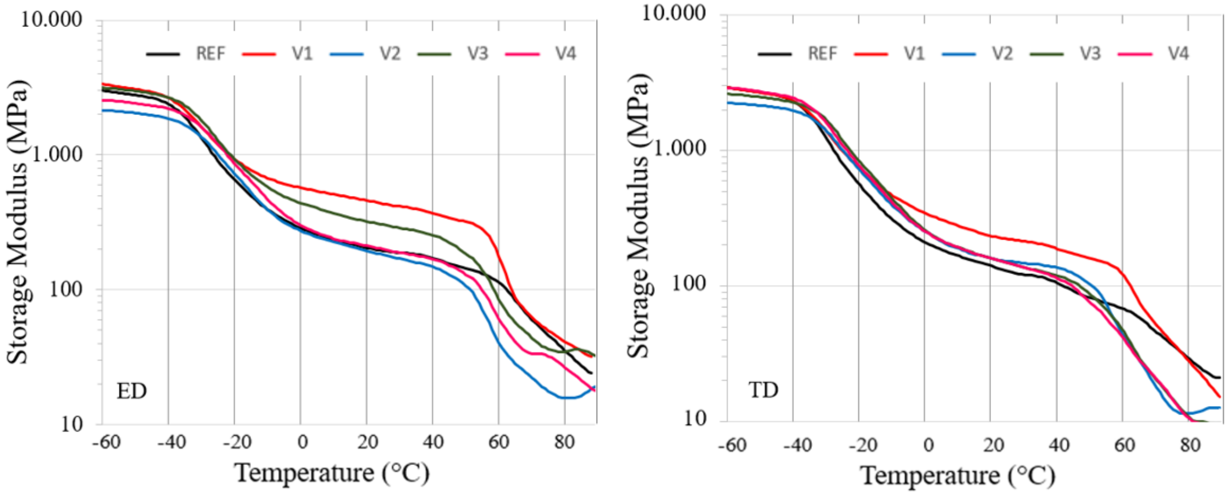

Figure 15: Comparison of temperature dependent logarithmic storage moduli [log(E'(T, ω=1Hz)] of REF, V1 to V4 in ED (left) and TD (right). (Paper II)

Figure 16 shows the comparison of temperature dependent loss factor (*tan δ*) of REF and V1 to V4 in ED and TD at 1 Hz.

Tan δ at $T_{g,ss}$ shows a decrease of values in ED for V1 to V4 compared to REF. In contrast, at $T_{g,hs}$ *tan δ* shows a shift to lower temperatures. Also, the exact same effect is also seen in TD. This indicates that CECL reactions preferably take place in the soft segment phase.

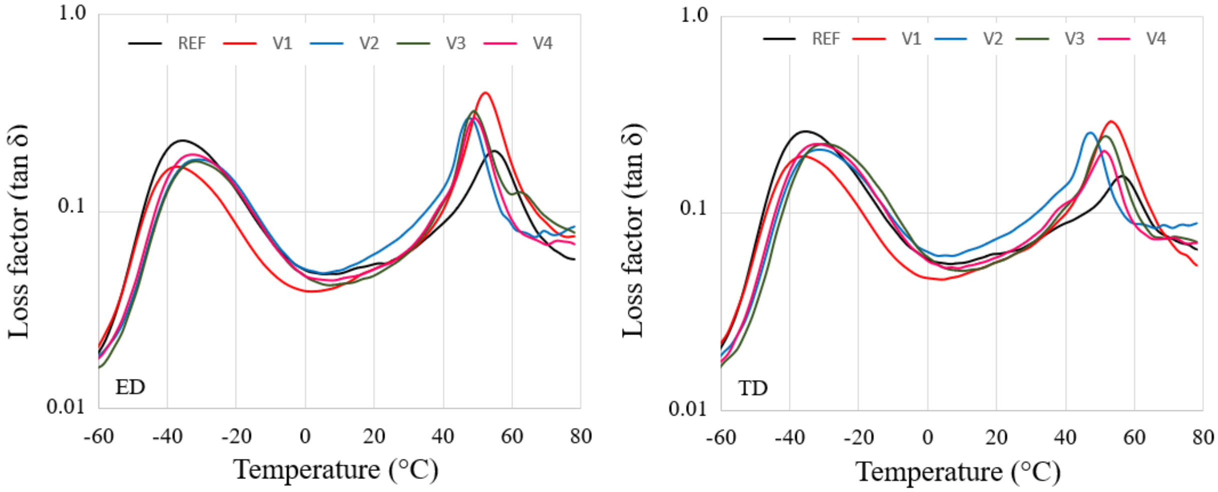

Figure 16: Comparison of temperature dependent loss factor of REF, V1 to V4 in ED (left) and TD (right) at 1 Hz. (Paper II)

Evaluating the DMA measurements in detail, Table 7, for REF and V1 the $T_{g,ss}$ (E''_{max}) coincide, whereas they are shifted for V2 to V4 by 3 to 5 K towards higher temperatures indicating cross-linking in soft segment phases. Interestingly, $T_{g,hs}$ of

V1 to V4 are decreased by 2 to 4 K, respectively, compared to REF. This is in contrast to the DSC data, where $T_{g,hs}$ of V1 to V4 increased by 7 to 8 K. This can be explained by the fact that films shrink freely in the DSC experiment reducing the free volume and shifting $T_{g,hs}$ to higher temperatures. Shrinkage is prevented in the DMA experiment due to the sample clamps and the free volume is maintained at least at the beginning of softening.

Table 7 Storage moduli *E'* and loss moduli *E''*, glass temperatures of soft segments $T_{g,ss}$ and glass temperatures of hard segments $T_{g,hs}$ determined using maxima of *E''* and *tan δ* of REF and V1 to V4 compounds evaluated at 1 Hz. (Paper I)

Sample		***E'***	***E''***	$T_{g,ss}$ **(*E''*)**	$T_{g,hs}$ **(*E''*)**	$T_{g,ss}$ **(*tan δ*)**	$T_{g,hs}$ **(*tan δ*)**
		MPa	MPa	°C	°C	°C	°C
REF	ED	177±33	10.3±1.2	-41.7±0.2	52.4±0.8	-35.5±0.1	54.8±0.7
	TD	124±13	8.0±1	-41.9±0.1	55.0±0.4	-35.2±0.1	56.7±0.3
V1	ED	387±38	21.0±1.4	-41.7±0.6	50.6±1.2	-36.8±0.9	53.3±1.2
	TD	322±17	20.0±1.6	-41.9±0.1	51.0±0.1	-36.1±0.3	53.6±0.1
V2	ED	210±33	13.0±1.4	-38.8±0.7	50.0±4.2	-32.7±0.5	51.9±4.5
	TD	151±12	11.0±0.8	-38.9±0.9	50.0±1.3	-32.2±0.9	52.1±1.1
V3	ED	184±15	9.3±1.2	-36.8±0.7	50.5±5.8	-31.0±0.5	52.5±6.2
	TD	126±5	7.3±0.5	-37.2±0.5	53.6±3.8	-30.6±0.5	56.1±4.0
V4	ED	270±24	15.0±1.9	-38,7±1.3	50.0±4.3	-32.9±1.9	52.0±4.4
	TD	133±6	8.7±0.9	-38.0±0.4	49.6±5.7	-31.8±0.8	51.8±6.1

According to DMA data, V1 hardly affected the T_g values of both segments, whereas other CECLs caused the T_g to increase in the soft segment phase and a decrease in the hard segment phase. This means that cross-linking mainly occurred in the soft segment phase. In conclusion, cross-linking in the hard segment phase was found for V3 and V4 after processing.

4.1.3 Elongational properties

An evaluation using a Sentmanat Extensional Rheometer (SER) was performed (Paper IV). Prior to measurements of elongational viscosities using the SER device, two principal conditions should be checked: mild intensity of sample sagging during the process of temperature setting and an acceptably small deviation from exponential decrease of sample cross-sections.

Due to sagging, the precise of this quantity shortcomings cannot be determined. However, if we want to compare two materials – regardless of their geometrical form – using the SER device the term ´elongation ratio at film rupture´ (ER_{FR}) seems to be adequate and relates the time spans t_{rupt} that elapsed between a start of drum revolution with a fixed sample and a final film rupture for two samples 1 and 2

$$ER_{\mathrm{FR}} = \frac{t_{\mathrm{rupt,1}}}{t_{\mathrm{rupt,2}}} \tag{3}$$

First, it was necessary to determine the temperatures under which the SER device could be used for the investigated five PLA/PBAT blends. Based on the range between 135 °C and 170 °C it was found that the optimal common temperature interval is 150 ± 5 °C for the CECL modified blends V1 to V4, and for the material V4 even at higher temperatures. In this interval, all PLA/PBAT blends exhibited optimal balanced fluid-like behaviors with acceptable sagging. Nevertheless, the remaining deviations of individual optimal temperatures may worsen comparisons among sample characterizations using ER_{FR} a little bit. Only in the case of REF, the temperature had to be lowered to 140 °C due to intensive sagging at 150 °C.

The thermo-mechanical properties of blown films of REF, V1 to V4 are anisotropic (Paper I) because of orientation effects of dispersed droplets in the melt [75] and polymer chains both introduced during blown film extrusion [76].

The mean times to film rupture scattered less than 5 % for each extensional rate, and the TD values always exceeded those in ED, showing that the morphology formation differs with respect to ED and TD during the blown film process.

For REF and V1 to V4, there was measured a time interval that elapsed between the start of SER drums revolution and material rupture. All measurements were carried out for two widths of rectangular samples (transverse direction, 0°): 12.7 mm (maximum possible width in the SER device) and 9 mm. Each measurement was conducted at least in triplicate and the results as shown on Figure 17.

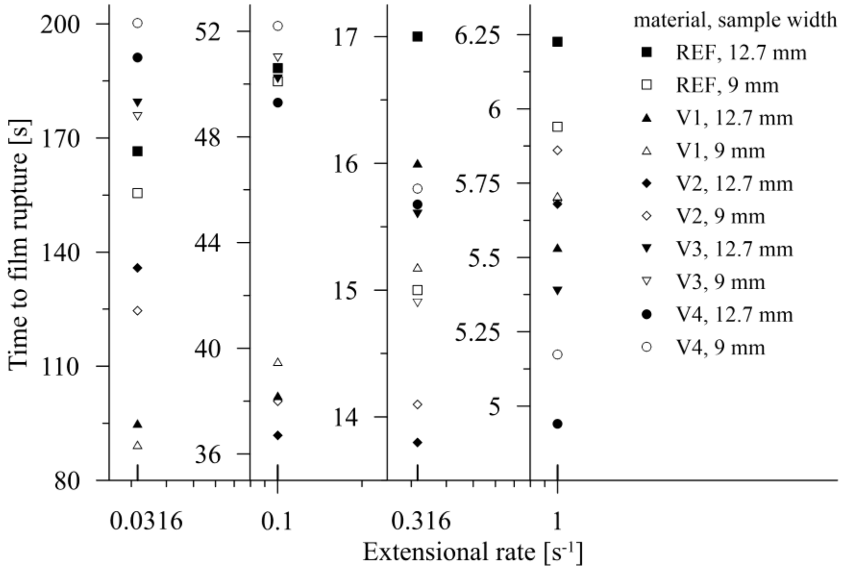

Figure 17: Elongational rate dependent times to film rupture in TD, individual charts. (Paper IV)

It is apparent that the initial macromolecular interplay for low extension rates favors disentanglement. It is replaced by consecutive passage to strain hardening where the rupture time intervals for pure PLA/PBAT blend significantly dominate. It is necessary to remind that REF was measured at 140°°C, i.e. by 10 °C lower than the modified samples V1-V4. This difference is suppressed for lower extension rates (as for 0.0316 s^{-1}) due to the process of disentanglement as discussed above.

With increasing extensional rates, strain hardening starts to compete and successively replaces the process of disentanglement. This can be demonstrated for REF at an extensional rate of 1 s^{-1} at 140 °C having the highest values of time to film rupture. However, at 150 °C REF exhibits a pronounced liquid-like behavior preventing elongation measurement. On the contrary, decreasing temperature by 10 °C reduces the liquid-like behavior of modified samples, which would reflect in apparent prolongation of breakage time (for instance by 17 % for V1, sample width 12.7 mm, extensional rate 1.0 s^{-1}).

The practical coincidence of the results expressed through a ratio relating the times to film fracture for both widths

$$R_{\mathrm{width}} = \frac{t_{\mathrm{rupt,12.7\ mm}}}{t_{\mathrm{rupt,9\ mm}}} \qquad (5)$$

documents an excellent homogeneity of the prepared materials without air bubbles and with initial uniform thickness due to good mixing during melt compounding. The dispersion of the ratio R_{width} is limited to the interval between 0.95 and 1.1, as seen on Figure 18, which corresponds to the experimental errors.

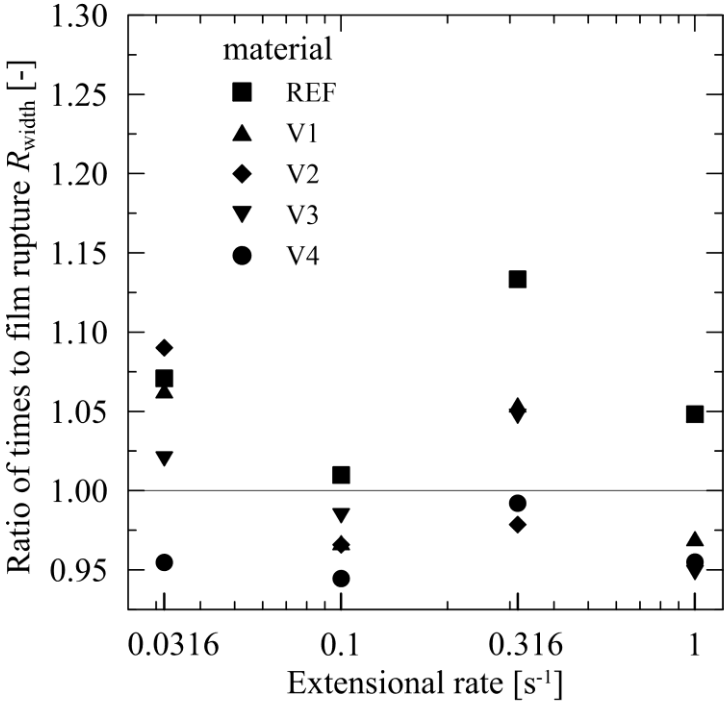

Figure 18: Ratios of times to film rupture of width 12.7 mm to width 9 mm. (Paper IV)

The result obtained for the modified blends corresponds to the molecular mass exhibited by the results from GPC (Paper III). The results showed significant increases in the molecular masses of V3 and V4 due to cross-linking reactions which correspond to findings based on the MVR measurements (Paper I). For V3 and V4 the number average molar mass nearly doubled that of REF (meaning that a single CECL molecule joins two polymer chains on average), whereas V1 and V2 have more or less identical molecular masses as REF. This indicates that in the case of V3 and V4 the CECL molecules react chemically with the polymer chains mainly forming a link between two macromolecules of PBAT on average. In the case of V1 and V2 the mean molecular masses are identical to REF. This may mean that CECL molecules hardly react with the PBAT molecules but cause chain scission of PLA molecules. Furthermore, a certain amount of the CECL may remain unreacted in V1 and V2. This explains the higher MVR values of V1 and V2 and does not exclude grafting reactions of CECL to macromolecules.

The obtained results justify the introduction of the quantity ´elongation ratio at film rupture ER_{FR}´, comparing elongational attributes of the modified blends.

4.2 Thermal properties

CECL process-induced structural changes were investigated with DSC.

Around 50 °C a glass transition of the hard segment $T_{\mathrm{g,hs}}$ occurs followed by an evaporation of tetrahydrofuran (THF) at 62 °C indicating chemical reactions of PBAT and PLA during compounding [77]. Furthermore, broad melting peaks for PBAT around 115 °C and for PLA around 150 °C are measured.

Evaluating the DSC traces in detail of the 1st, cooling and 2nd heating runs of REF and V1 to V4 in granules, Table 8, it can be seen that $T_{\mathrm{g,hs}}\_1$ of V1 to V4 decrease in relation to REF in the 1st run, meaning that the hard segments have higher mobility due to CECL induced reactions which increase distances between chains or leave unreacted CECL molecules acting as softeners. During the 2nd heating run, the $T_{\mathrm{g,hs}}\_2$ increased compared to the 1st heating run indicating further chemical reactions in the compound representing the extrusion process before film blowing. Concerning REF the $T_{\mathrm{g,hs}}\_2$ (onset) value of V1 is reduced from 55.9 °C to 51.1 °C indicating some chain scission or degradation in the hard segment phase. $T_{\mathrm{g,hs}}\_2$ (onset) for V2 is unaltered indicating no degradation, whereas $T_{\mathrm{g,hs}}\_2$ (onset) for V3 and V4 has increased from 55.9 °C to 58.4 °C and from 55.9 °C to 59.2 °C, respectively, indicating cross-linking.

The melting temperatures T_{m1}_1 of V1 to V4 show lower values than T_{m1}_1 (REF) of 113 °C indicating that CECL hinders the formation of thicker lamellae in PBAT. In the 2nd heating run, all compounds have the first melting temperatures T_{m1}_1 around 116 °C. The second melting temperature T_{m2}_1 of REF and V1 to V4 range between 150 °C and 153 °C indicating similar structures of the PLA phase in all compounds. Nevertheless, on the second melting temperature T_{m2}_*2* peaks are only found for REF and V2 signalling a suppressed PLA crystallization in V1, V3 and V4. The heats of fusion of V3 and V4 are in both heating runs smaller than in the REF showing that cross-linking reduces crystallinity. The crystallization enthalpy in the cooling runs exceeds the total heats of fusion (sum of both peaks) by 20 to 50 % which is surprising as they also exceed crystallization enthalpies. This can be explained by the superposition of the crystallization and glass transition of the hard segment.

Table 8 Glass temperature of hard segments $T_{g,hs}$, crystallization temperature T_{cr}, melting temperatures T_{m1} of PBAT and T_{m2} of PLA with corresponding heats of fusion ΔH_{m1} and ΔH_{m2} determined by 1st run, cooling run and 2nd run of DSC measurements of granules of REF and V1 to V4 compounds. (Paper I)

Prop.	**REF**	**V1**	**V2**	**V3**	**V4**
$T_{g,hs}$_*1* (°C)	50±0.03	43.7±2.02	46.7±0.08	47.8±0.27	46.2±0.07
T_{m1}_*1* (°C)	81.2±0.5	84.8±0.5	77.8±1.2	94.9±1.5	81.1±0.1
T_{m2}_*1* (°C)	143.2±0.8	144.2±0.2	143.4±0.7	142.7±1.5	143.2±0.6
T_{cr} (°C)	75.4±0.3	83.4±0.02	83.0±0.43	87.3±0.23	87.2±0.21
$T_{g,hs}$_*2* (°C)	55.9±0.28	51.1±2.1	54.9±0.86	58.4±0.46	59.2±1.5
T_{m1}_*2* (°C)	88.4±0.35	89.1±0	88.9±0.35	83.6±0.24	83.8±0.12
T_{m2}_*2* (°C)	143.8±0.3	-	144.0±0.12	-	-
ΔH_{m1}_*1* (J g^{-1})	8.5±0.17	9.4±0.6	6.9±0.6	5.1±0.15	5.2±0.75
ΔH_{m2}_*1* (J g^{-1})	0.3±0.08	1.1±0.18	1.9±0.04	1.1±0.5	2.8±0.12
ΔH_{cr} (J g^{-1})	11.0±0.3	11.6±0.13	10.9±0.2	9.1±0.12	10.3±0.09
ΔH_{m1}_*2*(J g^{-1})	7.3±0.2	7.3±0.16	5.8±0.14	5.8±0.28	5.8±0.05
ΔH_{m2}_*2* (J g^{-1})	0	-	0.8±0.05	-	-

An evaluation of the DSC traces for 25 µm films was also performed. Results for films of V1 to V4 exhibit similar behaviour as the granules: in the 1st heating run V3 and V4 have lower $T_{g,hs}$_*1* than V1 and V2, whereas in the 2nd heating run it is vice versa. This indicates that the amorphous hard segment phases of V3 and V4 are more disordered after film blowing probably due to incomplete chemical reactions.

The crystallization enthalpies during the cooling run of REF and V1 to V4 are higher than those of the granules, showing that the remaining preferential chain orientations due to the film blowing even in the melt after the first heating run easing and enabling subsequent crystallization [78].

The effects on thermal properties of REF, V1 to V4 with the variation of BUR were also evaluated, as seen in Table 9. The glass transition temperatures of the hard segments $T_{g,hs}$ decrease with BUR indicating higher molecular mobilities of the amorphous phases due to slightly larger mean chain distances caused by grafted CECL molecules. Only at BUR=3.5, V3 and V4 exhibit higher $T_{g,hs}$. Possibly polymer chains can better align with each other under a more pronounced biaxial orientation because of higher melt viscosities.

The PBAT melting peaks have widths of more than 30 °C indicating wide distributions of lamellae thicknesses. In that respect, the temperatures of the melting peaks T_{m1} provide insights into how the choice of BUR affects the lamellae growth during the crystallization of blown films and the achievable crystallinity. For all BUR, T_{m1} of V3 and V4 are lower than for REF, V1 and V2 indicating that higher molecular weights and melt viscosities shift the peaks to lower lamellae thicknesses. Furthermore, a strong dependency of T_{m1} is observed for BUR=2.5 with 5 to 15 °C decreased T_{m1}, and for BUR=3.5 with 1 to 5 °C increased T_{m1} compared to BUR=1.5. Interestingly no systematic change is observed for heats of fusions ΔH_{m1} indicating that the interplay of nucleation, crystal growth and film cooling is complex. This is stated by the crystallization temperatures T_{cr} and crystallization enthalpies ΔH_{cr} which both show no systematic BUR dependency.

Table 9 BUR dependency of thermal properties of REF, V1 to V4 in terms of glass temperature of hard segments $T_{g,hs}$, melting temperatures T_{m1} of PBAT and T_{m2} of PLA with corresponding heats of fusion ΔH_{m1} and ΔH_{m2} determined from 1st heating runs, crystallization temperature T_{cr}, and crystallization enthalpy ΔH_{cr} determined from cooling runs; temperature accuracy ΔT is ± 1 °C and enthalpy accuracy ΔH is 1 J/g. (Paper V)

	$T_{g,hs}$	T_{m1}	ΔH_{m1}	T_{m2}	ΔH_{m2}	T_{cr}	ΔH_{cr}
	°C	°C	J/g	°C		°C	J/g
	midpoint	PBAT	PBAT	PLA	PLA	peak	
			BUR 1.5				
REF	53	117	4.6	147	0.5	73	10.0
V1	57	120	3.9	151	1.7	83	11.9
V2	50	119	6.5	150	1.4	83	13.3
V3	49	113	5.9	149	1.0	71	12.3
V4	51	116	7.5	150	0.2	80	13.0
			BUR 3.5				
REF	48	122	4.2	149	0.5	87	13.6
V1	49	120	3.4	151	1.9	93	11.4

V2	48	125	8.5	149	1.9	93	13.7
V3	51	112	4.1	151	1.1	71	12.2
V4	50	119	5.6	151	0.7	79	12.9

These DSC results for the granules and films showed that the chemical reactions were incomplete after compounding and the film blowing intensified them, even for 25 µm films were being rapidly cooled. This behavior is explained by the CECL molecules being linked with one reactive site of polymer chains during compounding, while other reactive sites only show reactive possibilities if a chain slip occurs, such as in elongational flow during film blowing. For the evaluation with BUR, it is possible to conclude that the PLA phases crystallize during blown film extrusion under similar conditions for all BUR.

To confirm the interactions interpreted from DSC and mechanical analysis, FTIR-ATR was performed on the 25 µm blown films.

The functional groups of PBAT are described as peak at around 1710 cm^{-1} represents carbonyl groups (C=O) in the ester linkage, at 1265 cm^{-1} a peak intercepts C-O in the ester linkage, and at around 725 cm^{-1} a peak stand for methylene ($-CH_2-$) groups. Bending peaks of the benzene substitutes are located at wavenumbers between 700 and 900 cm^{-1}.

After CECL modification of the REF blend, the PLA band at 864 cm^{-1} is slightly shifted for V2, V3 and V4 to smaller wavenumbers up to 850 cm^{-1} indicating reactions, which enhance vibrations of the α-methyl group. A weak band occurring at 920 cm^{-1} is characteristic of unsaturated vinyl groups.

Overall, the spectra of V1 to V4 do not differ significantly from REF suggesting only small changes in the chemical structure of PBAT/PLA within the sensitivity limit of FTIR.

4.3 Process-induced morphology

In order to study the process-induced morphology, SEM of fracture surfaces of blown extrusion films were made, including BUR 1.5 and 3.5 (Paper II and V).

The fracture surfaces of REF, V1, and V4 clearly show the effects of BUR and CECL in both the ED and TD. All fracture surfaces at BUR=1.5 in ED exhibit a pronounced tough fracture behavior with a lot of PBAT fibrils, Figure 19, whereas in TD they appear rather brittle, Figure 6, although a few PBAT fibrils are visible, e.g. Figure 20 arrow 49. At BUR=2.5 and 3.5, all fracture surfaces exhibit an overall brittle fracture failure behavior, most pronounced for BUR=2.5. However, a few PBAT fibrils were found on all fracture surfaces, showing that the failure was not completely brittle, for example, Figure 19 arrows 8, 76, and 87 in the ED and Figure 20 arrows 12, 23, 77, 85, and 89. This indicates that the failure behavior is affected by the processing conditions in terms of the chosen BUR.

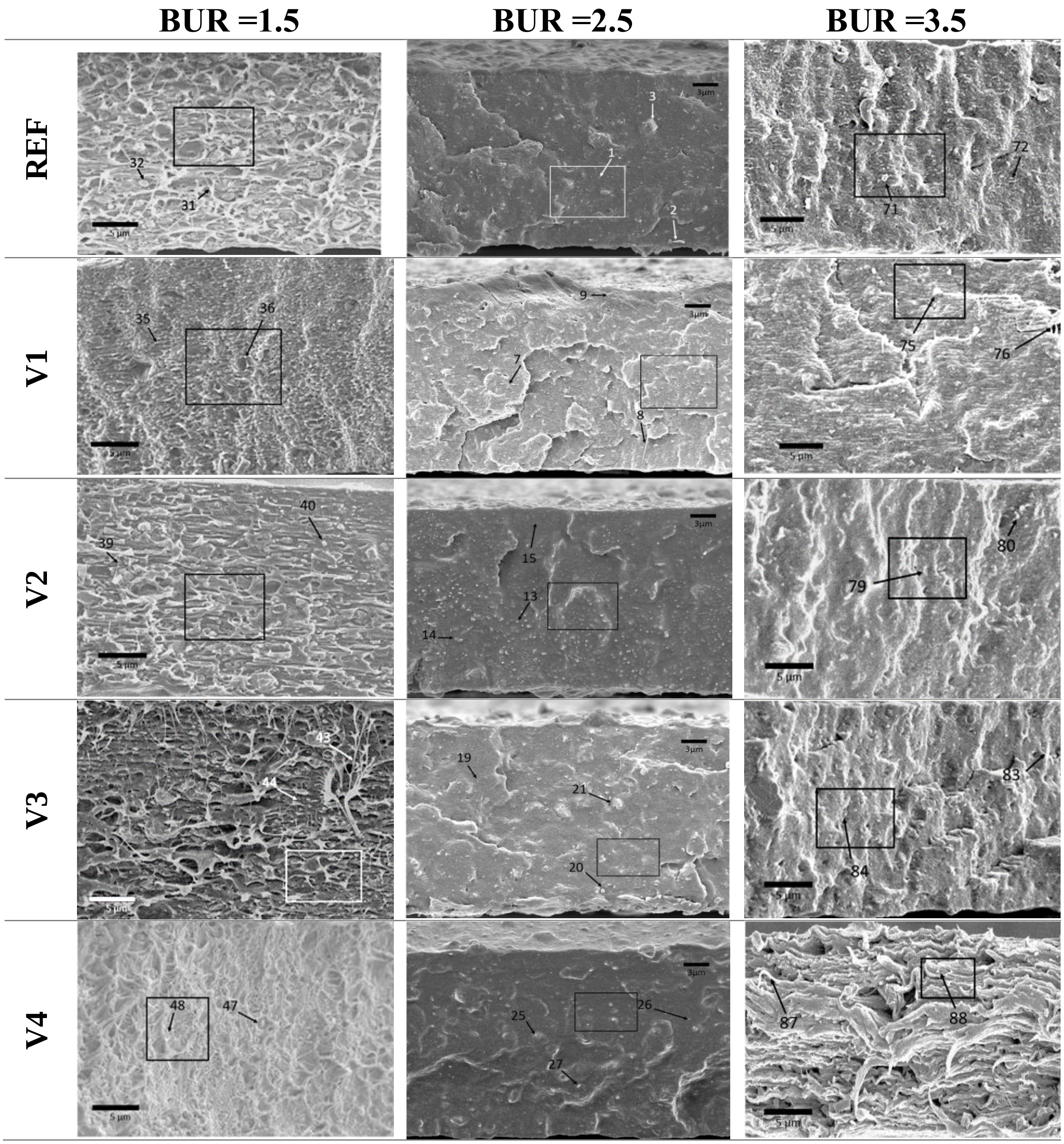

Figure 19: Effects of CECL on BUR dependent morphology of blown films of REF, V1 to V4 in ED, magnification 3,500. The rectangles represent the magnified areas displayed in Figure 21. (Paper II and V)

All brittle fracture surfaces exhibit "sea island structures," mainly in the core region, that consist of spherical PLA droplets without adhering PBAT, e.g. Figure 19 arrow 1, 20, 25, 71, 75, 84 and 88 in ED and Figure 20 arrow 4, 11, 16, 24, 28, 30, 38, 50, 78, 81 and 90 in TD, and spherical depressions in the PBAT matrix formed by PLA droplets, e.g. arrow 34 in ED and arrow 11, 24, 29 and 34 in TD, having typical diameters of 200 to 500 nm. Some spherical PLA droplets were also visible on the tough fracture surface in the ED at BUR=1.5, Figure 19 arrow 32, 40, and 47. This shows that the interface adhesion between PBAT and PLA is weak and that, in particular, the small PLA droplets remain almost un-deformed during blown film extrusion.

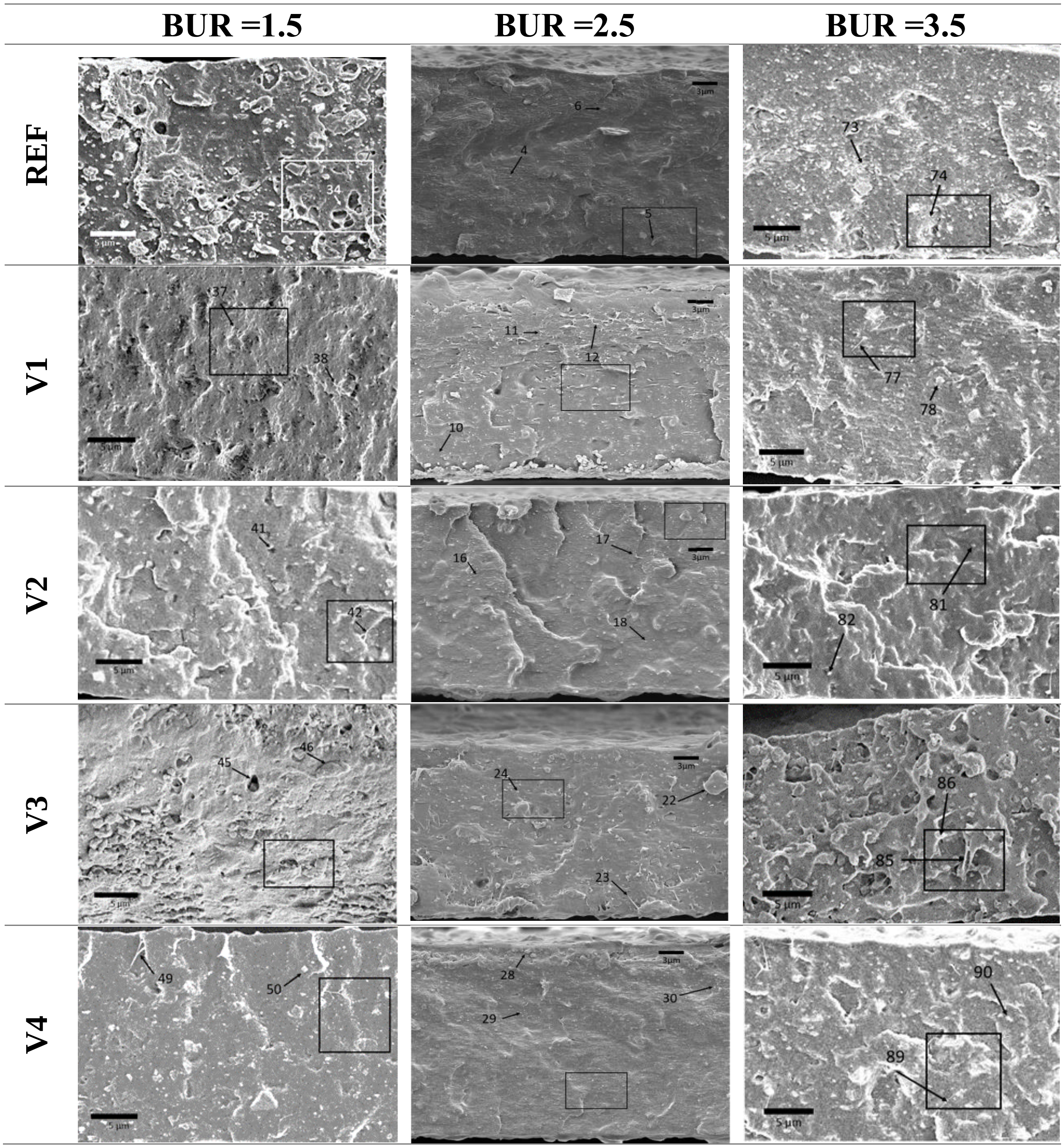

Figure 20: Effects of CECL on BUR dependent morphology of blown films of REF, V1 to V4 in TD, magnification 3,500. The rectangles represent the magnified areas displayed in Figure 22. (Paper II and V)

At the large magnification, the line structures become better visible on the fracture surfaces of REF, V1 and V2 in ED for BUR=2.5 and 3.5, Figure 21 e.g arrow 39, and REF, V1 to V4 in TD, Figure 22 e.g. arrow 35, 40 and 47.

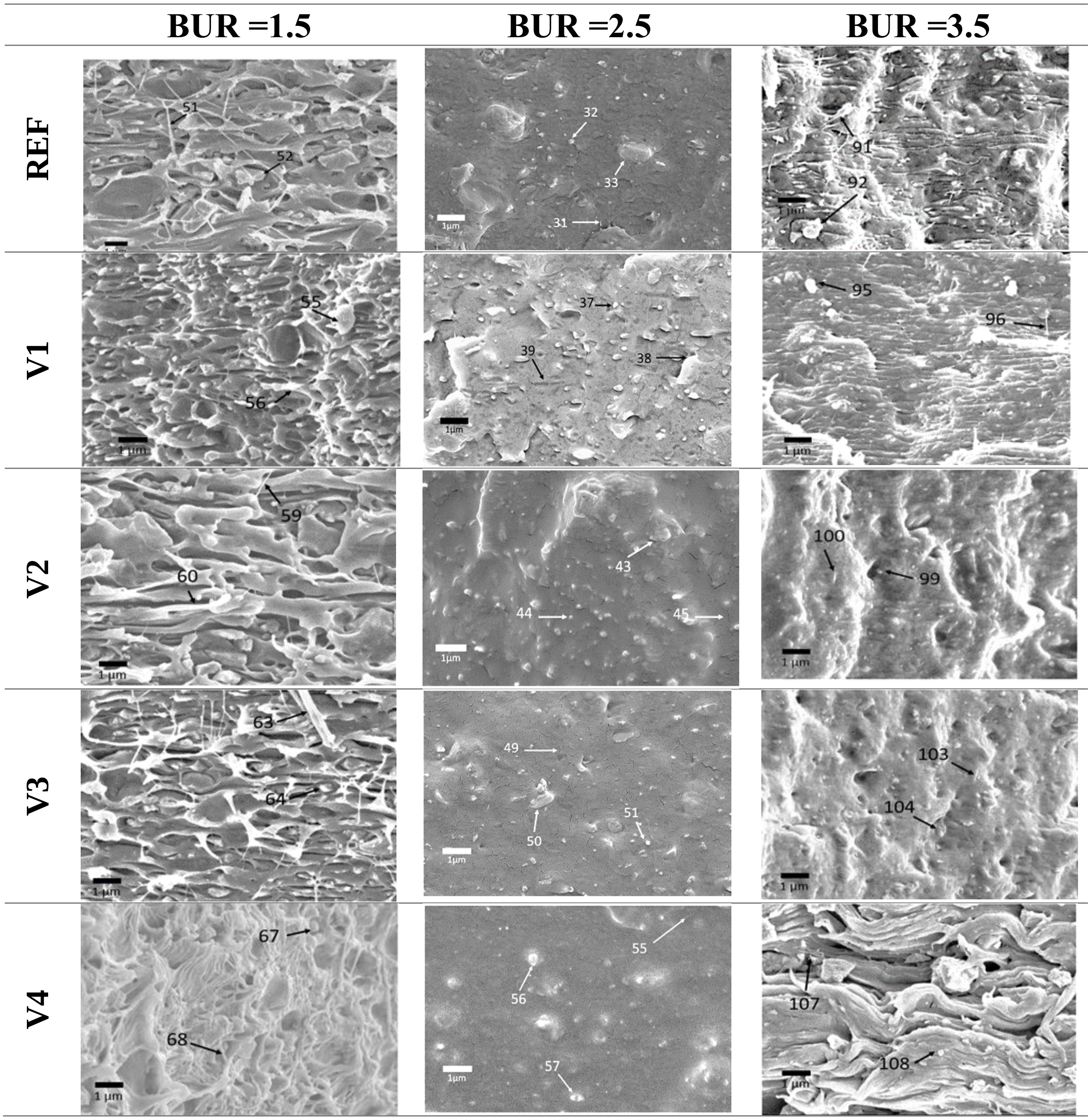

Figure 21: Effects of CECL on BUR dependent morphology of blown films of REF, V1 to V4 in ED, magnification 10,000. (Paper II and V)

These lines can be explained either by stretching large spherical PLA droplets to fine PLA fibrils or by directed lateral crystallization due to elongational flows during blown film extrusion. Even for BUR=1.5, the fracture surfaces in the ED clearly exhibited highly ductile deformations and many PBAT fibrils, as shown in Figure 21 (arrows 51, 56, 59, 63, and 68).

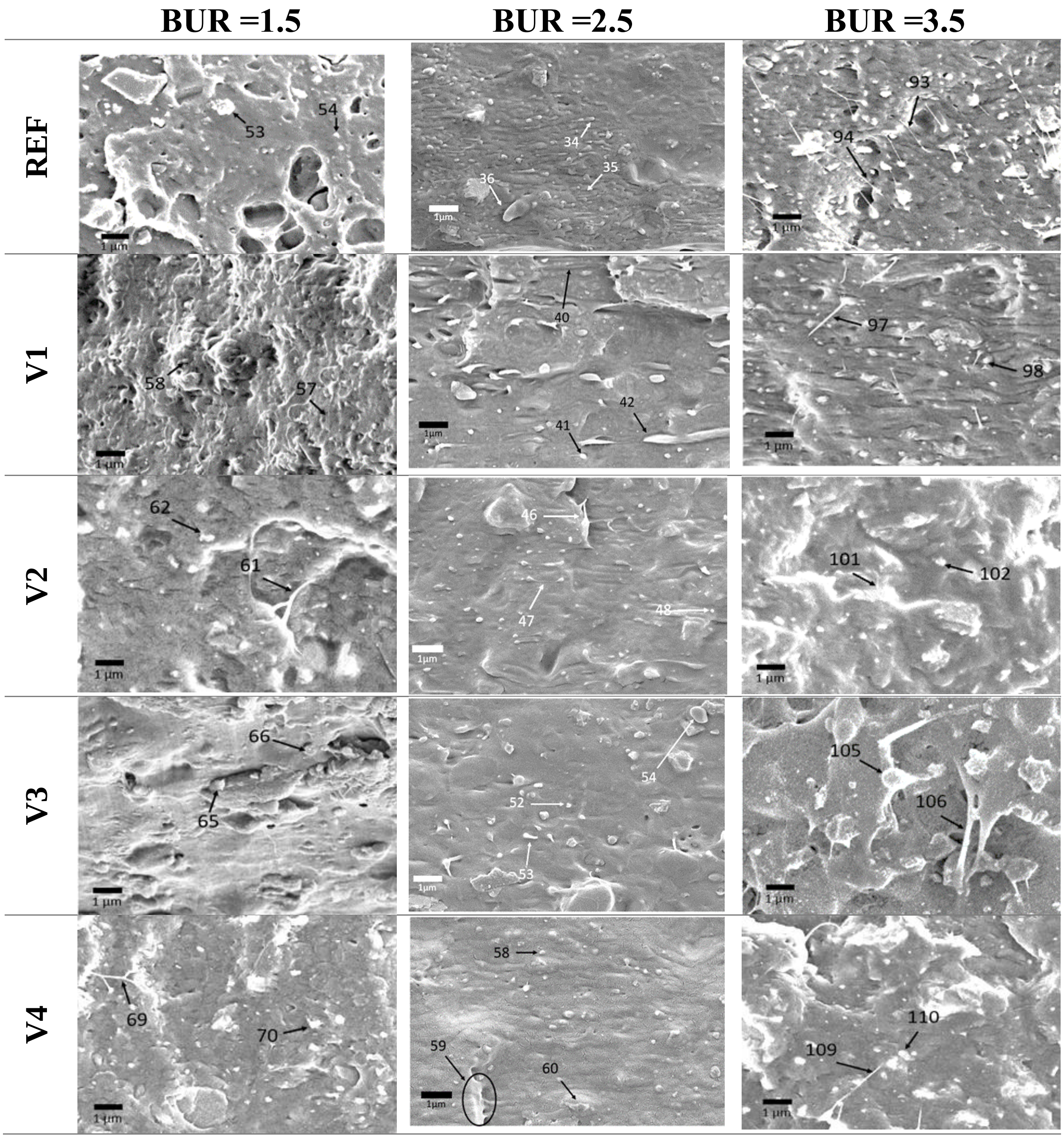

Figure 22: Effects of CECL on BUR dependent morphology of blown films of REF, V1 to V4 in TD, magnification 10,000. (Paper II and V)

At all BUR, undeformed spherical PLA droplets are clearly visible in the ED, as shown in Figure 21, for example, arrows 32, 33, 37, 44, 51, 56, 57, 64, 67, 92, 95, and 107, and in the TD, Figure 22 arrows 35, 48, 52, 58, 98, 102, and 110 for REF, V1 to V4. On the fracture surface of V2 in the TD, elongated PLA droplets and a

PLA fibril were visible (Figure 22, arrow 42). Interestingly, V4 is exhibited in the ED at BUR=3.5, which is a highly ductile fracture surface resembling a ruptured layer structure with embedded PLA droplets.

This ductile fracture behavior in the ED can be explained by the high DR of 18–19. The macromolecules in the melt are highly oriented in the ED but hardly oriented in the TD, which favors the growth of crystalline lamellae in the TD. This may create a pronounced shish-kebab morphology with a succession of crystalline and amorphous lamellae in the ED. At BUR=1.5, the polymer molecules were only slightly oriented in the TD, and crystal lamellae growth in the ED hardly occurred. Amorphous lamellae can provide considerable ductility, as they are not stiffened by crystalline cross-lamellae.

4.4 Disintegration in compost and their performance effect

4.4.1 Kinetics of disintegration behavior

The results of the disintegration trials will be presented and discussed in comparison between the different samples and their behavior under composting conditions in each trial series. The visual inspection of films shows that temperature has a significant effect on the disintegration behavior of the PBAT/PLA compounds modified by the CECLs (Paper III). At 30 °C, REF, V1 and V2 exhibit small stains on the surface which indicate a starting disintegration after 2 months. At 30 °C PLA is in a glassy state (glass temperature of 60 °C) preventing its degradation.

At 60 °C, REF exhibits a mean disintegration after 7 days, V1 and V2 a severe one, whereas V3 shows starting disintegration, and V4 still seems to be unaffected. The states of disintegration are in line with the increased melt flow ratios due to chain scission of V1 and V2 compared to REF, and the decreased melt flow ratios of V3 and V4 showing cross-linking (Paper I).

By evaluating the relative mass at 30 °C for 8 weeks for REF, V1 to V4, was possible to see that it is relatively unchanged in the range of the scatter of the mass determination, indicating that the disintegration processes have not led to mass decreases yet. The mass disturbances can be attributed to processes, that occur within the initiation time, e.g. mass increase due to chemical reactions, humidity uptake and remaining compost particles or mass decrease due to the release of degradation reaction or loss of microplastics during cleaning.

At 60 °C the relative mass remains relatively unchanged only for 4 days. Afterwards, for V1 and V2 a pronounced mass decrease is observed. REF exhibits a less pronounced mass decrease between days 5 and 6. V3 shows a tendency of decreasing mass, whereas V4 seems not to disintegrate even after 7 days. This shows that the initiation time is significantly affected by the chosen CECL, and the chemical changes induced with CECL.

Because of the scatter of the mass measurements, the disintegration becomes confirmed only if the masses have decreased to less than 90 % of the initial mass (Paper III). After 8 weeks at 30 °C, the REF lost 4 %, and 7 % after 7 days at 60 °C (Paper III). The decrease of V1 and V2 exceeds that of REF showing that the biodegradation of V1 and V2 was more proceeded. For V3 and V4 the decrease is less than for REF showing that crosslinking hinders biodegradation and decelerates disintegration. However, the decreases are still within the scatter of the relative masses during the initiation times. This indicates further that the mass may increase at first due to the uptake and generation of low molecular weight components during the initiation times of storage in compost in addition to adherent compost particles.

The films stored in compost at 60 °C were further investigated with respect to their disintegration kinetics by determining the cross-sectional areas of the holes in the films after storage in compost to elucidate the kinetic parameters initiation time t_{init} and disintegration time τ_{disint} of REF, V1 to V4. The experimental data can be fitted by equation (Paper III) with reasonable R^2, Table 10, although the fitting assumes only a single dominating disintegration process.

Table 10 Kinetic parameters of REF and V1 to V3 compounds over 7 days at 60 °C of disintegration in compost.

Kinetic Parameters		**Compound**			
	Unit	REF	V1	V2	V3
Time to 80 % of initial mass $t_{0.8}$	h	132.7	105.6	105.8	174.1
Initiation time t_{init}	h	32.8	34.1	23.7	45.8
Disintegration time τ_{disint}	h	385.1	147.3	94.8	1179.5
R^2 of fits		0.96	0.95	0.97	0.83

The times to the mass decrease of 80 % $t_{0.8}$ exceed the initiation times t_{init} by a factor 3 to 4, Table 14. This indicates that the initiation time of the disintegration process depends on the mass and that the holes in the films may occur before the significant mass changes. In the case of the increasing cross-sectional areas of the holes during the storage in compost, several processes might be involved (an uptake of humidity, settlement of micro-organisms on a film surface, chemical modification of polymers, and chain scissions) before the metabolizing of the polymer segments really begins.

Clearly, some degree of disintegration happened before the occurrence of the first holes. The disintegration times τ_{disint} show that the CECL significantly affects the disintegration processes. The disintegration rate of V1 and V2 exceeds that of REF by factors 2.5 and 4, respectively, whereas it is decreased to 0.25 for V3. Regarding V4, as mentioned above, it did not show any holes within 7 days, so it was not evaluated.

It’s possible to conclude that even small amounts of the added CECL significantly alter the disintegration and degradation behavior of REF depending on whether it causes chain scission or crosslinking. Polymer chains have to be segmented to metabolizable lengths by e.g. hydrolytic degradation before biodegradation can start.

4.4.2 Disintegration effect on mechanical kinetics

Evaluation was carried out on the film samples during the storage of REF, V1 to V4 in compost for 8 weeks at 30 °C (Paper III). At first, it led to an increase in Young’s modulus before they slowly decreased again. This increase can be explained by annealing and/or post-crystallization effects in the amorphous phase of PLA. As PLA is the disperse phase here, it is protected by the PBAT matrix against degradation at the beginning of compost storage at 30 °C. Therefore, the increases of PBAT moduli may occur already at 30 °C as humidity leads to more mobile polymer chains, and thus enabling a slow post-crystallization. After 2 weeks, E was at highest in ED, while in 4 weeks the highest was achieved in TD indicating that the degradation processes during the initiation time affect E in ED and TD in a different manner. This means that the orientation of polymer chains and the sites, that enable hydrolytic and microbial degradation, differ in ED and TD. Thus, during the starting phase, one direction is more affected by biodegradation than the other for the given number of degradation reactions.

Regarding the tensile strengths, for REF, V1 and V2 a continuous decrease in ED was found, whereas V3 and V4 exhibited a plateau of tensile strength for 4 weeks before a decrease of 60 to 70 %. The plateau behavior of tensile strengths for 4 weeks was observed for all compounds in TD combined with a slightly more pronounced subsequent strength decrease in the order of 10 %. Similar behavior was also found for the elongations at break. This concludes that tensile strength and elongation at break are very sensitive to structural changes prior to visible mechanical disintegration. This is confirmed by the fact that the V3 and V4 were cross-linked by the CECLs and exhibited reduced tensile strengths and elongations at break and after compost storage for 4 to 8 weeks at 30 °C, despite no visible disintegration. For V1 and V2, the effect of chain scission is confirmed.

With compost storage at 60 °C, has a significantly more pronounced impact on mechanical properties. However, annealing effects cannot occur anymore as the amorphous phase of PLA is now in the liquid state. The E of V1 and V2 in ED and TD were decreased respectively, after 7 days, and close to zero after 14 days, whereas Young’s modulus plateaus were observed for REF (3 days), V1 and V2 (14 days) followed by a decrease of 60 % (REF) after 7 days, 70 % (V3) and 20 % (V4) after 28 days. Young’s modulus plateaus were found for REF (3 days) with a fast decrease close to zero after 7 days, V3 (14 days) with a decrease of 60 % after 28 days, and V4 (28 days) with no decrease in TD.

The tensile strengths in ED and TD of REF, V1 and V2 were continuously decreased after 7 days. The decreases for V3 and V4 were 70 and 60 %, respectively, after 28 days. Only V4 exhibited an initial strength plateau during 2 to 3 days. The elongations at break in ED and TD of V1 and V2 decreased continuously close to zero after 7 and 3 days, respectively, REF and V3 exhibited a plateau for 1 day before decreasing close to zero after 7 days and 28 days, respectively. Only V4 showed a plateau for 3 days before decreasing by 80 % in ED and close to zero in TD.

The changes of tensile strengths and elongation at break indicate that these properties are more sensitive with respect to degradation and disintegration processes.

It's possible to conclude that REF, V1 to V4 have been mechanically degraded already during compost storage at 30 °C, but visibly these processes were still on an initiation level with negligible effects on film masses. At 60 °C. the degradation processes were significantly accelerated as REF, V1 and V2 were already severely disintegrated after 7 days (Paper III) and both tensile strengths and elongations at break dropped to low values.

4.4.3 Disintegration effect on mean molecular masses

Further GPC was used to check if molecular degradation has occurred during compost storage, Table 10. The results confirm the earlier findings of MVR measurements that the CECL cause cross-linking in V3 and V4 as their molecular masses ($M_n \approx 75{,}000$ g/mol) are roughly doubled compared to REF. REF, V1 and V2 with molecular masses around 44,000 g/mol showed that the CECL did not significantly change the molecular masses and as a consequence the macromolecular structure. Most of CECL molecules have to be remained as low molecular components in the polymer. chain scission. The significantly higher MVR values of V1 and V2 compared to REF in Paper I were explained by chain scission. However, according to the GPC results, Table 11, this cannot be the reason for the higher MVR values. They have to be explained by an enhancement of the melt flowability provided the remaining unreacted CECL as low molecular components [79].

Compost storage at 30 °C did not change the molecular mass of REF, V1, V3 and V4 with respect to the accuracy of the measurement. Only V2 exhibited further cross-linking with increased molecular masses in the order of 10 %. Compost storage at 60 °C led to molecular degradation of REF and V1 after 7 days, and also to further cross-linking of V2 in the order of 10 %. For V3 and V4 molecular degradation was not detected either at 30 °C nor at 60 °C.

Table 11 Determination of the mean molecular masses due to GPC measurements with number-average molecular mass M_n, weight-average molecular mass M_w, and polydispersity index of the polymer PDI; accuracy of measurements is 2,000 g/mol for M_n and 3,000 g/mol for M_w., after compost storage for defined time.

Compound	M_n	M_w	**PDI**
	g/mol	g/mol	
Initial state			
PBAT	43,000	107,000	2.45
REF	44,000	83,000	1.89
V1	42,000	81,000	1.92
V2	46,000	92,000	1.98
V3	75,000	149,000	1.99
V4	72,000	141, 000	1.95
PLA	218,000	309, 000	1.42

	M_n	M_w	**PDI**	M_n	M_w	**PDI**
	g/mol	g/mol		g/mol	g/mol	
After storage for 2 weeks at 30 °C				**After storage for 8 weeks at 30 °C**		
REF	46,000	86,000	1.89	43,000	82,000	1.94
V1	47,000	87,000	1.88	43,000	83,000	1.92
V2	52,000	105,000	1.99	51,000	103,000	2.00
V3	75,000	160,000	2.12	78,000	162,000	2.07
V4	75,000	148,000	1.98	74,000	148,000	2.01
After storage for 3 days at 60 °C				**After storage for 7 days at 60 °C**		
REF	41,000	80,000	1.95	34,000	67,000	1.97
V1	42,000	79,000	1.90	37,000	71,000	1.93
V2	52,000	99,000	1.91	49,000	96,000	1.97
V3	72,000	154,000	2.14	72,000	154,000	2.13
V4	71,000	141,000	1.98	72,000	143,000	1.99

The GPC results clearly show that under the given composting conditions molecular degradation started only after 3 days at 60 °C for REF and V1. This means that the determined mass losses and the growth of the hole area have to be caused by mechanical disintegration towards micro-plasticization.

5. CONCLUSION

In this thesis, the process-induced changes in thermo-mechanical viscoelastic properties and the corresponding morphology of biodegradable polybutylene adipate terephthalate (PBAT) and polylactic acid (PLA) blown film blends modified with various multifunctional chain-extending cross-linkers (CECL) was investigated.

The modification of the PBAT/PLA blend (REF) with the four different CECLs has modified the properties significantly. Tris(2,4-di-tert-butylphenyl)phosphite and 1,3-phenylenebisoxazoline act rather as flow enhancers without changing the molecular masses, evidenced by the gel permeation chromatography (GPC), while aromatic polycarbodiimide and poly(4,4-dicyclohexylmethanecarbodiimide) led to cross-linking. Further, process-induced changes are different for the extrusion direction (ED) and the direction transverse to extrusion (TD). This has been reflected in the elongation at break in ED and tear resistance in TD decreased, whereas elongation at break in the TD and tear resistance in the ED remain unaltered.

Thermal evaluation (with differential scanning calorimetry - DSC) for the granules and films exhibited that the chemical reactions were incomplete after compounding and that film blowing intensifies them, even for 25 µm films being rapidly cooled. This behavior is explainable by the molecules being linked with one reactive site of polymer chains during compounding, while other reactive sites only show reaction possibilities if a chain slip occurs, such as in elongational flow during film blowing.

According to DMA data, tris(2,4-di-tert-butylphenyl)phosphite hardly affected the glass transition temperature (T_g) values of either segment, whereas other CECLs caused increases in the soft segment phase and decreases in the hard segment phase. This meant that cross-linking occurred in the soft phase, whereas CECL reactions occurred in the hard phase only with increased free volume or CECL.

With the Fourier-transform infrared spectroscopy (FTIR), the PLA band (864 cm^{-1}) was shifted for 1,3-phenylenebisoxazoline, aromatic polycarbodiimide and poly(4,4-dicyclohexylmethanecarbodiimide) to a smaller wavenumber length indicating interactions between PBAT/PLA and these CECLs during the compounding process. From the scanning electron microscopy (SEM) of the unmodified and modified blown extrusion films, the circular/spherical PLA dispersed phase was observed. When PLA starts to crystallize at temperatures below 130 °C, then thus freezes in the current geometry. The spherical PLA particles in the melt are not more stretched in ED than in TD direction due to the substantial large draw ratio than blow-up ratio (BUR), creating the occurrence of PLA fibrils happening only in the TD direction. The investigation with 2 different BURs (1.5 and 3.5) has shown that the PLA droplets with diameters of 200-500 nm solidify shortly after being extruded from the die and remain undeformed during blowing.

This means that the PLA droplets represent thermoplastic filler particles in the blown films and that the PBAT matrix experiences all deformations. This relates to the mechanical performance showing the elongation at break and tear strength in TD to decrease systematically with BUR, whereas an arbitrary dependence was obtained for other properties such as Young's modulus, tensile strength, and seal strength. The anisotropic morphology introduced during film blowing has presented its effects during the degradation processes. Their disintegration behavior was significantly altered concerning the unmodified reference blend. Finally, in the process of blown film extrusion, the elongational behavior represents a very important characteristic. However, its evaluation may be quite often problematic, and its accuracy dramatically differs from that of shear viscosity. By using an SER Universal Testing Platform, results have shown that for very low extensional rates, an elongational process is dominated by disentanglement of the studied materials preventing strain hardening. By comparing the rupture time intervals, it is possible to evaluate mutually the chosen materials. It was confirmed that out of four chain-extending cross-linkers, the best contribution to blown film processing was exhibited by poly(4,4-dicyclohexylmethanecarbodiimide).

To conclude, this work has brought more and better insight into how process-induced properties of PBAT/PLA blends function with modified CECLs and the synergy of it with blow-film processing by evaluating the main characteristics to improvement for the packaging industry.

6. CONTRIBUTION TO SCIENCE AND PRACTICE

Bioplastics make it possible to develop innovative, alternative solutions compared to conventional plastics. Biodegradable plastics allow enhanced end-of-life scenarios for disposal and recycling. The packaging industry is currently the largest user of bioplastics, but there are many other suitable applications possible, and consumers are increasingly interested in alternative bio-solutions. To reach this goal, materials have to be improved and optimized in terms of processing-induced properties, to achieve the right balance of performance. A better understanding of the processing-induced properties will lead to optimized blend films.

This PhD thesis is focused on the question of how process-induced properties are affected by the introduction of four different CECLs. A comprehensive study on the influence of reactive extrusion (compounding) aligned with different blow-up ratios on the blown film extrusion was performed. To interpret the results, several models/ideas are presented because direction comparison to the results of other researchers could not be made due to the lack of literature correlating specific behaviors and their conjugated effects of CECL influenced with processing (anisotropy in extrusion/transversal directions). The following topics of this PhD thesis are considered the most important contribution to both science and practice:

1. The investigation of the effects of four multifunctional chain-extending cross-linkers on the processability, mechanical performance, and structure of PBAT and PLA blends to provide an insight into the reactive extrusion of different functional groups and their effect on mechanical and thermal performance and morphological effects.
2. The insight of the different blow-up ratio and the comparison with the mechanical and morphological performance to determine the correct set-up to provide the best suitable end-use.
3. The study of extension characteristics by using an SER Universal Testing Platform provides good insight that elongation behavior represents an important characteristic in the blown film extrusion process, thus leading to a better understanding of extensional rates and their correlation to the strain hardening behavior.

REFERENCES

[1] https://www.ifbb-hannover.de/files/IfBB/downloads/faltblaetter_broschueren/Biopolymers-Facts-Statistics_2016.pdf, last access 13 Dezember 2021

[2] F.P.L. Mantia, L. Botta, M.C. Mistretta, A.D. Fiore, V. Titone, Investigation on the properties and on the photo-oxidation behaviour of polypropylene/fumed silica nanocomposites, *Polymers* 12 (2020), 2297

[3] M. Shen, B. Song, G. Zeng, Y. Zhang, W. Huang, X. Wen, W. Tang, Are biodegradable plastics a promising solution to solve the global plastic pollution?, *Environ. Pollut.* 263 (2020), 114469

[4] T. Narancic, K. O'Connor, Plastic waste as a global challenge: are biodegradable plastics the answer to the plastic waste problem?, *Microbiology* 165 (2018), 129-127

[5] L. Yu, K. Dean, L. Li, Polymer blends and composites from renewable resources, *Prog. Polym. Sci.* 31 (2006), 576-602

[6] R. Muthuraj, M. Misra, A. K. Mohanty, Biodegradable poly(butylene succinate) and poly(butylene adipate-co-terephthalate) blends: reactive extrusion and performance evaluation, *J. Polym. Environ.* 22 (2014), 336-349

[7] S.Y. Gu, K. Zhang, J. Ren, H. Zhan, Melt rheology of polylactide/poly(butylene adipate-co-terephthalate) blends, *Carb. Polym.* 74 (2008), 79-85

[8] U. Witt; R.J. Müller, W.-D. Deckwer, Biodegradation of Polyester Copolymers Containing Aromatic Compounds, *J. Macr. Sci. A* 32 (1995) 851–856

[9] H. Tsuji, Poly(lactide) stereocomplexes: formation, structure, properties, degradation, and applications, *Macromol. Biosci.* 5 (2005), 569–597

[10] E.C.D. Nunes, A.G. Souza, R.D.S. Coiado, E.A.B. Moura, D.S. Rosa, Evaluation of the poly (lactic acid) and calcium carbonate effects on the mechanical and morphological properties in PBAT blends and composites, *Int. J. Inn. Sci. Eng. Tech.* 4(6) (2017), 313-318

[11] M. Shahlari, S. Lee, Mechanical and morphological properties of poly(butylene adipate-co-terephthalate) and poly(lactic acid) blended with organically modified silicate layers, *Polym. Eng. Sci.* 52 (7) (2012), 1420-1428

[12] W. M. Aframehr, B. Molki, P. Heidarian, T. Behzad, M. Sadeghi, R. Bagheri, Effect of calcium carbonate nanoparticles on barrier properties and biodegradability of polylactic acid, *Fibers Polym.* 18 (2017), 2041-2048

[13] B. Wang, Y. Jin, K. Kang, N. Yang, Y. Weng, Z. Huang, S. Men, Investigation on compatibility of PLA/PBAT blends modified by epoxy-terminated

branched polymers through chemical micro-crosslinking, *e-Polymer* 20 (2020), 39–54

[14] S. Su, M. Duhme, R. Kopitzky, Uncompatibilized PBAT/PLA blends: manufacturability, miscibility and properties, *Materials* 13 (2020), 4897

[15] R. Al-Itry, K. Amnawar, A. Maazouz, Improvement of thermal stability, rheological and mechanical properties of PLA, PBAT and their blends by reactive extrusion with functionalized epoxy, *Polym. Degr. Stab.* 97 (2012) 1898–1914

[16] W. Dong, B. Zou, Y. Yan, P. Ma, M. Chen, Effect of chain-extenders on the properties and hydrolytic degradation behavior of the poly(lactide)/poly(butylene adipate-co-terephthalate) blends, *Int. J. Mol. Sci.* 14 (2013), 20189–20203

[17] L. C. Arruda, M. Megaton, R. E. S. Bretas, M. N. Ueki, Influence of chain extender on mechanical, thermal and morphological properties of blown films of PLA/PBAT blends, *Polym. Test.* 43 (2015), 27–37

[18] H. Pan, Z. Li, J. Yang, X. Li, X. Ai, Y. Hao, H. Zhang, L. Dong, The effect of MDI on the structure and mechanical properties of poly(lactic acid) and poly(butylene adipate-co-butylene terephthalate) blends, *RSC Adv.* 8 (2018), 4610–4623

[19] M. Lackner, F. Ivanič, M. Kováčová, I. Chodák, Mechanical properties and structure of mixtures of poly(butylene-adipate-coterephthalate) (PBAT) with thermoplastic starch (TPS), *Int. J. Biobased Plast.* 3 (2021), 126–138

[20] https://docs.european-bioplastics.org/publications/fs/EUBP_FS_Packging.pdf, last access 18th Dezember 2021

[21] P. Suwanamornlert, N. Kerddonfag, A. S. W. Chinsirikul, W. Zhou, V. Chonhencho, Poly(lactic acid)/poly(butylene-succinate-co-adipate) (PLA/PBSA) blend films containing thymol as alternative to synthetic preservatives for active packaging of bread, *Food Packag. Shelf Life* 25 (2020), 100515

[22] B. Palai, S. Mohanty, S. K. Nayak, Synergistic effect of polylactic acid (PLA) and poly (butylene succinate-co-adipate) (PBSA) based sustainable, reactive, super toughened eco-composite blown films for flexible packaging applications, *Polym. Test.* 83 (2020), 106130

[23] J. Jian, Z. Xiangbin, H. Xianbo, An overview on synthesis, properties and applications of poly(butylene-adipate-co-terephthalate)–PBAT, *Polym. Adv. Technol.* 3 (2020), 19-26

[24] U. Witt, R. J. Müller, W.-D. Deckwer, Biologisch abbaubare Polyester-Copolymere mit einstellbaren Anwendungseigenschaften auf Basis

chemischer Massenprodukte, *Chemie Ingenier Technik* 67 (7) (1995), 904-907

[25] U. Witt, R. J. Müller, W.-D. Deckwer, Biodegradation of Polyester Copolymers Containing Aromatic Compounds, *J. Macromol. Sci.* A32 (4) (1995), 851-856

[26] J. Verena, Packaging related properties of commercially available biopolymers - an overview of the status quo, *EXPRESS Polym. Lett.* 12 (2018), 429-435

[27] J. Ahmed, S. K. Varshney, Polylactides—chemistry, properties and green packaging technology: A Review, *Int. J. Food Prop.* 14:1 (2011), 37-58

[28] R. Song, M. Murphy, C. Li, K. Ting, C. Soo, Z. Zheng, Current development of biodegradable polymeric materials for biomedical applications, *Drug Des. Dev. Ther.* 12 (2018) 3117—3145

[29] H. Liu, J. Zhang, Research progress in toughening modification of poly(lactic acid), *J. Polym. Sci. B: Polym. Phys.* 49 (2011), 1051–1083

[30] L. Jiang, M. P. Wolcott, J. Zhang, Study of biodegradable polylactide/poly(butylene adipate-co-terephthalate) blends, *Biomacromolecules* 7 (2006), 199-207

[31] S. Auras, L. T. Lim, S. Selke, H. Tsuji, Poly(lactic acid): synthesis, structures, properties, processing and applications, 2010, Wiley-VCH, ISBN 978-0-470-64984-8

[32] W. Pivsa-Art, S. Pavasupree, N. O-Charoen, U. Insuan, P. Jailak, S. Pivsa-Art, Preparation of Polymer Blends Between Poly (L-Lactic Acid), Poly (Butylene Succinate-Co-Adipate) and Poly (Butylene Adipate-Co-Terephthalate) for Blow Film Industrial Application, *Energy Procedia* 9 (2011), 581-588

[33] I. Fortelny, A. Ujcic, L. Fambri, M. Slouf, Phase structure, compatibility, and toughness of PLA/PCL blends: a review, *Front. Mater.* 6 (2019), 206

[34] https://www.scanfill.se/de/uber-uns/produktion/, last access 16th Dezember 2021

[35] https://www.scanfill.se/de/uber-uns/produktion/, last access 16th Dezember 2021

[36] S. Y. Zhou, H. D. Huang, X. Ji, D. X. Yan, G. J. Zhong, B. S. Hsiao, Z. M. Li, Super-robust polylactide barrier films by building densely oriented lamellae incorporated with ductile in situ nanofibrils of poly(butylene adipate-co-terephthalate), *Appl. Mater. Interfaces* 8 (2016), 8096-8109

[37] E. J. Dil, P. J. Carreau, B. D. Favis, Morphology, miscibility and continuity development in poly(lactic acid)/poly(butylene adipate-co-terephthalate) blends, *Polymer* 68 (2015), 202-212

[38] L. W. Mckeen, Permeability Properties of Plastics and Elastomers, 2016, 4th. Elsevier, ISBN 978-0-323-50859-9

[39] https://www.appropedia.org/Blown_film_extrusion, last access 31st October 2021

[40] S. A. Ashter, Introduction to Bioplastics Engineering, 2016, 1st. Elsevier, ISBN 978-0-323-39396-6

[41] K. CANTOR, Blown Film Extrusion, 2011, 2nd. Hanser Fachbuchverlag, ISBN 978-1-569-90696-5

[42] S. Su, M. Duhme, R. Kopitzky, Uncompatibilized PBAT/PLA blends: manufacturability, miscibility and properties, *Materials* 13(21) (2020), 4897

[43] R. Hernandez, S. Selke, J. Culter, Plastics packaging: properties, processing, applications, and regulations, 2000, 2nd. Hanser Fachbuchverlag, ISBN 978-1-569-90822-8

[44] L. Jiang, M. P. Wolcott, J. Zhang, Study of biodegradable polylactide/poly (butylene adipate-co-terephthalate) blends, *Biomacromolecules* 7 (2006), 199-207

[45] https://elmendorfteartester.com/, last access 31 October 2021

[46] A. Pietrosanto, P. Scarfato, L. Di Maio, M. Nobile, L. Incarnato, Evaluation of the suitability of poly(Lactide)/poly(butylene-adipate-co-terephthalate) blown films for chilled and frozen food packaging applications, *Polymers* 12 (2020), 12, 804

[47] D. Kim, J. Lee, D. Lee, K. Seo, Plasticization effect of poly(lactic acid) in the poly(butylene adipate-co-terephthalate) blown film for tear resistance improvement, *Polymers* 12 (2020), 1904

[48] N. Mazzola, C. A. Cáceres, M. P. França, S. V. Canevarolo, Correlation between thermal behaviour of a sealent and heat sealing of polyolefin films, *Polym. Test.* 31(7) (2012), 870-875

[49] N. Z. Qureshi, E. V. Stepanov, G. Capaccio, A. Hiltner, E. Baer, Self-Adhesion of Polyethylene in the Melt. 1. Heterogeneous Copolymers, *Macromolecules* 34(5) (2001), 1358-1364

[50] R. Y. Tabasi, Z. Najarzadeh, A. Ajji, Development of high performance sealable films based on biodegradable/compostable blends, *Ind. Crops Prod.* 72 (2015), 206-213

[51] V. Thirtha, R. Lehman, T. Nosker, Morphological effects on glass transition behavior in selected immiscible blends of amorphous and semicrystalline polymers, *Polymer* 47(15) (2006), 5392-5401

[52] A. Carbonell-Verdu, J. Ferri, F. Dominici, T. Boronat, L. Sanchez-Nacher, R. Balart, L. Torre, Manufacturing and compatibilization of PLA/PBAT binary blends by cottonseed oil-based derivatives, *EXPRESS Polym. Lett.* 12(9) (2018), 808-823

[53] V. Ojijo, S. S. Ray, R. Sadiku, Toughening of biodegradable polylactide/poly(butylene succinate-co-adipate) blends via in situ reactive compatibilization, *ACS Appl. Mater. Interfaces* 5(10) (2013), 4266-4276

[54] J. Liu, L. Lou, W. Yu, R. Liao, R. Li, and C. Zhou, Long chain branching polylactide: structures and properties, *Polymer* 51 (2010), 5186–5197

[55] R. Al-Itry, K. Lamnawar, and A. Maazouz, Reactive extrusion of PLA, PBAT with a multi-functional epoxide: Physico-chemical and rheological properties, *Eur. Polym. J.* 58 (2014), 90–102

[56] X. Ai, X. Li, Y. Yu, H. Pan, J. Yang, D. Wang, H. Yang, H. Zhang, and L. Dong, The mechanical, thermal, rheological and morphological properties of PLA/PBAT blown films by using bis(tert-butyl dioxy isopropyl) benzene as crosslinking agent, *Polym. Eng. Sci.* 59 (2019), E227–E236

[57] J. Meissner, Stress and recovery maxima in LDPE melt elongation, *Polym. Bull.* 1 (1979), 397-402

[58] J. Meissner, and J. Hostettler, A new elongational rheometer for polymer melts and other highly viscous liquids, *Rheol. Acta* 33 (1994), 1-21

[59] H. Münstedt, New universal extensional rheometer for polymer melts. Measurements on a polystyrene sample, *J. Rheol.* 23 (1979), 421-436

[60] M. L. Sentmanat, Miniature universal testing platform: From extensional melt rheology to solid state deformation behavior, *Rheol. Acta* 43 (2004), 657-669

[61] D. Wu, A. Huang, J. Fan, R. Xu, P. Liu, G. Li, S. Yang, Effect of blending procedures and reactive compatibilizers on the properties of biodegradable poly(butylene adipate-co-terephthalate)/poly(lactic acid) blends, *J. Polym. Eng.* 41(2) (2021), 95-108

[62] Y. Deng, C. Yu, CP. Wongwiwattana, N. Thomas, Optimising ductility of poly (lactic acid)/poly (buthylene adipate-co-terephthalate) blends through co-continuous phase morphology, *J. Polym. Environ.* 26 (2018), 3802–3816

[63] N. Lucas, C. Bienaime, C. Belloy, M. Queneudec, F. Silvestre, J. E. Nava-Saucedo, Polymer biodegradation: Mechanisms and estimation techniques, *Chemosphere* 73 (2008), 429–442

[64] N. L. Davison, F. Barrère-de Groot, D. W. Grijpma, Degradation of biomaterials, *Tissue Engineering* (2014), 177–215

[65] A. Soroudi, I. Jakubowicz, Recycling of bioplastics, their blends and biocomposites: a review, *Eur. Polym. J.* 49 (2013), 2839–2858

[66] S. Tolga, S. Kabasci, M. Duhme, Progress of disintegration of polylactide (PLA)/poly(butylene succinate) (PBS) blends containing talc and chalk inorganic fillers under industrial composting conditions, *Polymers* 13(1) (2021), 10

[67] S. -R. Lee, H. -M. Park, H. Lim, T. Kang, X. Li, W. -J. Cho, C. -S. Ha, Microstructure, tensile properties, and biodegradability of aliphatic polyester/clay nanocomposites, *Polymer* 43 (2002), 2495–2500

[68] G. Kale, R. Auras, S. P. Singh, R. Narayan, Biodegradability of polylactide bottles in real and simulated composting conditions, *Polym. Test.* 26 (2007), 1049–1061

[69] BIO-FED Website, TDPG of M·VERA® B5029. https://bio-fed.com/fileadmin/bio-fed/PDFs/BIO-FED_TDPG_MVERA_B5029_B0155_2023-03-09.pdf, last access 12 October 2022

[70] SONGWON Website, SONGNOXTM product description. Available online: https://www.songwon.com/products/songnox-1680, last access 12 October 2022

[71] SpecialChem Website, Technical Datasheet of 1,3-Phenylene-bis-oxazoline. Available online: https://polymer-additives.specialchem.com/product/a-evonik-1-3-phenylene-bis-oxazoline, last access 12 October 2022

[72] Lanxess Website, Technical Datasheet of Stabaxol® P110. Available online: https://lanxess.com/en/Products-and-Brands/Products/s/STABAXOL--P-110, last access 12 October 2022

[73] Nisshinbo Chem Website, Product Details of CarbodiliteTM HMV-15CA. Hydrolysis stabilizer for polyesters including Biodegradable resin. Available online:https://www.nisshinbo-chem.co.jp/english/products/carbodilite/poly.html, last access 12 October 2022

[74] A. Soroudi, I. Jakubowicz, Recycling of bioplastics, their blends and biocomposites: a review, *Eur. Polym. J.* 49 (2013), 2839–2858

[75] R. Salehiyan, M. Nofar, K. Malkappa, S. S. Ray, Effect of nanofillers characteristics and their selective localization on morphology development and rheological properties of melt-processed polylactide/poly(butylene adipate-co-terephthalate) blend composites, *Polym. Eng. Sci.* 60 (2020), 2749–2760.

[76] S. Su, M. Duhme, and R. Kopitzky, "Uncompatibilized PBAT/PLA blends: Manufacturability, miscibility and properties," Materials 13, 4897 (2020).

[77] T. R. Rigolin, L. C. Costa, M. A. Chinellato, P. A. R. Muñoz, S. H. P. Bettini, Chemical modification of poly(lactic acid) and its use as matrix in poly(lactic acid) poly(butylene adipate-co-terephthalate) blends, *Polym. Test.* 63 (2017), 542–549

[78] T. Gong, R. Y. Bao, Z. Y. Liu, B. H. Xie, M. B. Yang, W. Yang, The effect of chain mobility on the coarsening process of co-continuous, immiscible

polymer blends under quiescent melt annealing, *Phys. Chem. Chem. Phys.* 19 (2017), 12712-12719

[79] Y. Fu, G. Wu, X. Bian, J. Zeng, Y. Weng, Y, Biodegradation Behavior of Poly(Butylene Adipate-Co-Terephthalate) (PBAT), Poly(Lactic Acid) (PLA), and Their Blend in Freshwater with Sediment, *Molecules* 25 (2020), 3946

LIST OF FIGURES

LIST OF TABLES

	PDI; accuracy of measurements is 2,000 g/mol for M_n and 3,000 g/mol for M_w. (Paper III)
Table 7	Storage moduli *E’* and loss moduli *E’’*, glass temperatures of soft segments $T_{g,ss}$ and glass temperatures of hard segments $T_{g,hs}$ determined using maxima of *E’’* and *tan* δ of REF and V1 to V4 compounds evaluated at 1 Hz. (Paper I)
Table 8	Glass temperature of hard segments $T_{g,hs}$, crystallization temperature T_{cr}, melting temperatures T_{m1} of PBAT and T_{m2} of PLA with corresponding heats of fusion ΔH_{m1} and ΔH_{m2} determined by 1st run, cooling run and 2nd run of DSC measurements of granules of REF and V1 to V4 compounds. (Paper I)
Table 9	BUR dependency of thermal properties of REF, V1 to V4 in terms of glass temperature of hard segments $T_{g,hs}$, melting temperatures T_{m1} of PBAT and T_{m2} of PLA with corresponding heats of fusion ΔH_{m1} and ΔH_{m2} determined from 1st heating runs, crystallization temperature T_{cr}, and crystallization enthalpy ΔH_{cr} determined from cooling runs; temperature accuracy ΔT is ± 1 °C and enthalpy accuracy ΔH is 1 J/g. (Paper V)
Table 10	Kinetic parameters of REF and V1 to V3 compounds over 7 days at 60 °C of disintegration in compost.
Table 11	Determination of the mean molecular masses due to GPC measurements with number-average molecular mass M_n, weight-average molecular mass M_w, and polydispersity index of the polymer PDI; accuracy of measurements is 2,000 g/mol for M_n and 3,000 g/mol for M_w, after compost storage for defined time.

ABBREVIATIONS

AA	Adipic acid
ATR	Attenuated Total Reflectance
BDO	Butane diol
BUR	Blow-up ratio
CECL	Chain extending cross-linkers
CO_2	Carbon dioxide
CTE	Coefficient of thermal expansion
DIN	Deutsches Institut für Normung (in English, German Institute for Standardisation)
DCP	Dicumyl peroxide
DMA	Dynamic mechanical analysis
D-PLA	Poly(D-lactic acid)
DR	Draw ratio
DSC	Differential scanning calorimetry
ED	Extrusion direction
ETBP	Epoxy terminated branched polymer
FTIR	Fourier-transform infrared spectroscopy
GPC	Gel permeation chromatography
H_2O	Water
HDPE	High density polyethylene
HIPS	High impact polystyrene
IR	Infrared
ISO	International Standard Organization
IUPAC	International Union of Pure and Applied Chemistry
LDPE	Low density polyethylene
L-PLA	Poly(L-lactic acid)
MDI	4,4 methylene diphenyl diisocyanate
MVR	Melt Volume Rate
OL	Organosolv lignin
PA 6	Polyamide 6
PBAT	Polybutylene adipate terephthalate
PDI	Polydispersity index

PBS	Polybutylene succinate
PCL	Polycaprolactone
PDLA	Poly(D,L-lactic acid)
PE	Polyethylene
PHA	Polyhydroxyalkanoate
PHB	Polyhydroxybutyrate
PHV	Polyhydroxyvalerate
PLA	Polylactic acid
PP	Polypropylene
PS	Polystyrene
PTA	Terephthalic acid
SAXS	Small-angle X-ray scattering
SEM	Scanning electron microscopy
SER	Sentmanat Extensional Rheometer
TD	Transverse direction
THF	Tetrahydrofuran
WAXS	Wide-angle X-ray scattering
wt.%	Weight percentage

SYMBOLS

c_p	Heat capacity
E	Young‘s modulus
E'	Storage modulus
E''	Loss modulus
ε_{break}	Strain at break
F_{break}	Rupture force
F_{seal}	Seal strength
F_{tear}	Tear resistance
L	Length
M_n	Number molecular mass
M_w	Weight molecular mass
T	Temperature

$tan\delta$	Loss factor
T_{cr}	Crystallization temperature
T_{end}	End temperature
T_g	Glass transition temperature
$T_{g,hs}$	Glass temperature of hard segments
$T_{\mathrm{g,ss}}$	Glass temperature of soft segments
T_m	Melting temperature
T_{m1}	Melting temperature of PBAT
T_{m2}	Melting temperature of PLA
T_{start}	Starting temperature
W	Width
ΔH_{cr}	Crystallization enthalpy
ΔH_m	Melting enthalpy
ΔH_{m1}	Melting enthalpy of PBAT
ΔH_{m2}	Melting enthalpy of PLA
η_E	Elongational viscosity
σ_f	Fracture stress
σ_f	Fracture stress
σ_{max}	Tensile strength
ρ	Density
λ	Heat conductivity

PUBLICATIONS

Publications in context of this doctoral work:

- J. V. C. Azevedo, E. R. Dorp, B. Hausnerová, B. Möginger, The Effects of Chain-Extending Cross-Linkers on the Mechanical and Thermal Properties of Poly(butylene adipate terephthalate)/Poly(lactic acid) Blown Films. *Polymers* 13 (2021) 3092.
- J. V. C. Azevedo, E. R. Dorp, R. Grimmig, B. Hausnerová, B. Möginger, Process-Induced Morphology of Poly(Butylene Adipate Terephthalate) /Poly(Lactic Acid) Blown Extrusion Films Modified with Chain-Extending Cross-Linkers. *Polymers* 14 (2022) 1939.
- J. V. C. Azevedo, B. Hausnerová, B. Möginger, T. Šopík, Effect of chain extending crosslinkers on disintegration behavior of composted PBAT/PLA blown films. *Int. J. Mol. Sci.* 24 (2023) 4525.
- P. Filip, B. Hausnerová, B. Möginger, J. V. C. Azevedo, Improvement of elongational behavior of poly(lactic acid)/poly(butylene adipate terephthalate) blends in blown film extrusion using chain extending cross-linkers. Submitted to *Int. J. Biol. Macromol.,* November 2023, November 2023.
- J. V. C. Azevedo, E. R. Dorp, C. Kössler, C. Thomser, T. Šopík, B. Möginger B. Hausnerová, Blow molding-induced structure and performance of renewable PLA/PBAT packaging films modified with chain-extending cross-linkers. Submitted to *J. Ind. Eng. Chem.*, November 2023.

CURRICULUM VITAE

Date and place of birth: April 14th, 1988 in Guimarães, Portugal

Permanent Address: Nattermannallee 1, 50829 Köln, Germany

Education:

since 10/2018 – PhD studies at Thomas Bata University Zlín, Faculty of Technology, Department of Production Engineering

10/2006-12/2011 – Integrated Master's Degree in Polymer Engineering at Minho's University, Portugal, Faculty of Engineering

02/2010-07/2010 – ERASMUS-Sócrates Project at École de Mines de Douai, France

03/11-12/2011 – Master's degree thesis at 3B's Research Group in Biomaterials, Biodegradable and Biomimetics, Portugal

Work experience:

03/2012-11/2012 – Polymer Engineer at LKP, Lda, in Portugal

05/2013-04/2014 – Laboratory and Technical Office Support at Metabolix GmbH in Germany

10/2014-01/2023 – R&D Development Engineer at BIO-FED, a branch of AKRO-PLASTIC GmbH in Germany

02/2023 - present – Group Leader R&D and QA at BIO-FED, a branch of AKRO-PLASTIC GmbH in Germany

Fields of interest:

Bioplastics, biodegradable polymers, compounding

Juliana Vanessa Cardoso Azevedo, Ph.D.

Zpracování PBAT/PLA směsí: vliv procesních podmínek na strukturní a užitné vlastnosti

Manufacturing of Blends based on Biopolyesters and Polylactides: Process-induced Structure and Properties

Doctoral Thesis Summary

Published by: Tomas Bata University in Zlín,

nám. T. G. Masaryka 5555, 760 01 Zlín.

Edition: published electronically

Typesetting by: Juliana Vanessa Cardoso Azevedo, Ph.D.

This publication has not undergone any proofreading or editorial review.

Publication year: 2024

First Edition

ISBN 978-80-7678-228-0